

Chapter 9

Gold Nanoparticles: A Lethal Nanoweapon Against Multidrug-Resistant Bacteria



Md. Monir Hossain, Shakil Ahmed Polash, Tanushree Saha,
and Satya Ranjan Sarker

Abstract Multidrug-resistant (MDR) bacteria, also called superbugs, pose serious threat to the human health and existence because of their ability to develop resistant mechanism against commercially available antibiotics. Besides increasing the morbidity and mortality rate of patients, MDR bacteria are also putting huge financial stress on health sectors across the globe. It is estimated that approximately 700,000 people are losing their life every year due to MDR bacteria. It has been projected that more than 10 million people around the world will be the victim of MDR bacteria by 2050, if the current trend continues, superseding cancer as the main cause of global mortality. Hence, the mankind is in dire need to find an effective and safe tool against MDR bacteria.

Several metallic nanoparticles including Au, Ag, ZnO, and GO (graphene oxide) have shown antibacterial propensity against a wide range of bacteria. However, gold nanoparticles (AuNPs) received wide attention because of their inertness for the human body, easy surface fabrication properties, and optical properties. AuNPs demonstrate antibacterial activity through direct interaction with bacterial cell wall, generating reactive oxygen species (ROS), passing through the cell membrane and interacting with cellular macromolecules (i.e., DNA and proteins). In this chapter, we shall discuss different types of AuNPs, their role as potent antibacterial agents

M. M. Hossain · S. R. Sarker (✉)

Department of Biotechnology and Genetic Engineering, Jahangirnagar University,
Dhaka, Bangladesh

e-mail: satya.sarker@bgeju.edu.bd

S. A. Polash

Nano Biotechnology Research Laboratory (NBRL), School of Science, RMIT University,
Melbourne, VIC, Australia

T. Saha

Department of Textile Engineering, Dhaka University of Engineering and Technology,
Gazipur, Bangladesh

School of Engineering, RMIT University, Melbourne, VIC, Australia

against pathogenic as well as multidrug-resistant bacteria, mechanism of antibacterial activity, biocompatibility, and future prospects in healthcare system.

Keywords Gold nanoparticles · Multidrug-resistant bacteria · Antibacterial activity · Biocompatibility

9.1 Introduction

Gold (Au) is an inert metal with distinct electronic and optical properties. When Au nanoparticles (AuNPs) are excited with light of a particular wavelength, the incident photons interact strongly with the conduction band of electrons and cause them to oscillate with resonant frequency. The collective oscillation is known as localized surface plasmon resonance (LSPR) that creates strong and localized electromagnetic fields and allows sensitive detection of changes in dielectric environment surrounding the surface of nanoparticles. This unique property makes them highly useful in imaging, drug delivery, cancer theranostics, and tackling menace of multidrug-resistant bacteria (Shankar et al. 2004; Mukherjee et al. 2001; Li et al. 2014). Au nanoparticles induce hyperthermia (i.e., increased temperature to kill cancer cells) upon illumination with near-infrared (NIR) light (Dash and Bag 2014; Huang et al. 2011). Furthermore, AuNPs can also be successfully and selectively delivered to malignant as well as benign tumors and can act as carriers for chemotherapeutic drugs. They are used as imaging agents as well as biosensors because of their ability to emit photons upon illumination (Marangoni et al. 2013).

The misuse and overuse of antibiotics have resulted in the emergence of multidrug-resistant bacteria, which is the cause of an additional medical costs of up to billion dollars every year (Rossolini et al. 2014; Li et al. 2014). Hence, suitable antibacterial agents to deal with multidrug-resistant bacteria are urgently needed. The antibacterial activity demonstrated by various nanomaterials including Ag, Au, Cu, Ti, ZnO₂, and MgO₂ could be a suitable alternative to commercially available antibiotics (Vimbela et al. 2017; Hossain et al. 2019; Niloy et al. 2020; Polash et al. 2021; Ranjan Sarker et al. 2019). More specifically, gold nanoparticles (AuNPs) have distinctive properties including their adjustable shape, size, surface properties, optical properties, high stability, biocompatibility, and multiple functionalization potential that make them suitable for different applications in the field of nanomedicine (Ashraf et al. 2016).

Based on the unique physical and chemical properties of nanoparticles, they provide a common platform for therapeutic applications against drug-resistant bacteria (Li et al. 2014). For example, AuNPs have already been used in the treatment of gum disease and dental caries, diagnosis of cancer, and in tissue engineering. Since AuNPs have antifungal and antibacterial activity, they can be conjugated with

biopolymers to improve their efficacy as bioactive materials (Bapat et al. 2020). In addition, AuNPs can also be used as carriers of antibacterial drugs. Antibacterial drugs are conjugated with AuNPs through chemical interactions so that drugs can be released at the desired site of action (Fan et al. 2019). Notably, AuNPs do not show toxic effects to normal cells at certain concentrations (Fang et al. 2019; Chatterjee et al. 2011). Therefore, it is possible to modify AuNPs that exhibit antibacterial activity against standard bacterial strains in general and have unique antibacterial activity against multidrug-resistant bacteria in particular (Su et al. 2020).

The recent development in nanoscience and nanotechnology has helped researchers to design and develop novel biomaterials including AuNPs with excellent bioactivity as well as biocompatibility. Many inorganic (i.e., metal) nanoparticles have been developed including AuNPs. The AuNPs show various colors based on their shape, size, and amount of aggregation of particles (Daniel and Astruc 2004). They are used in medical and pharmaceutical industries for various purposes: antibacterial agents, antibiofilm, diagnostic tools, drug delivery vehicles, personal care products, and for cosmetics development (Su et al. 2020; Abdalla et al. 2020). This chapter summarizes recent research works on the development of AuNPs and their application to tackle the menace of pathogenic and multidrug-resistant (MDR) bacteria.

9.2 Different Types of AuNPs

There are many different types of gold nanoparticles (AuNPs) depending on their size, shape, and physical properties (Fig. 9.1). Important AuNPs include Au nanospheres, nanorods, nanoshells, and nanocages. There is also another type of Au-based nanoparticles known as “SERS nanoparticles” with excellent surface-enhanced Raman scattering property. Most of the AuNPs are produced with well-defined size, shape, and monodispersity due to the continuous development of synthetic, and characterization techniques in the last two decades.

9.2.1 *Au Nanospheres*

The gold nanospheres, also known as gold colloids of 2 to 100 nm in diameter, can be synthesized through controlled reduction of an aqueous HAuCl_4 solution using different reducing agents under varying conditions. Citrate is the most widely used reducing agent that can produce nearly monodisperse gold nanospheres (Turkevich et al. 1951; Frens 1973). The size of the nanospheres can be controlled by changing the citrate to gold ratio. Generally, less amount of citrate generates larger nanospheres. The two major limitations of this method are the low yield and the obligation of using water as the solvent. A two-phase method, introduced by Faraday in 1857, capable of producing stable (irrespective of temperature and air) gold

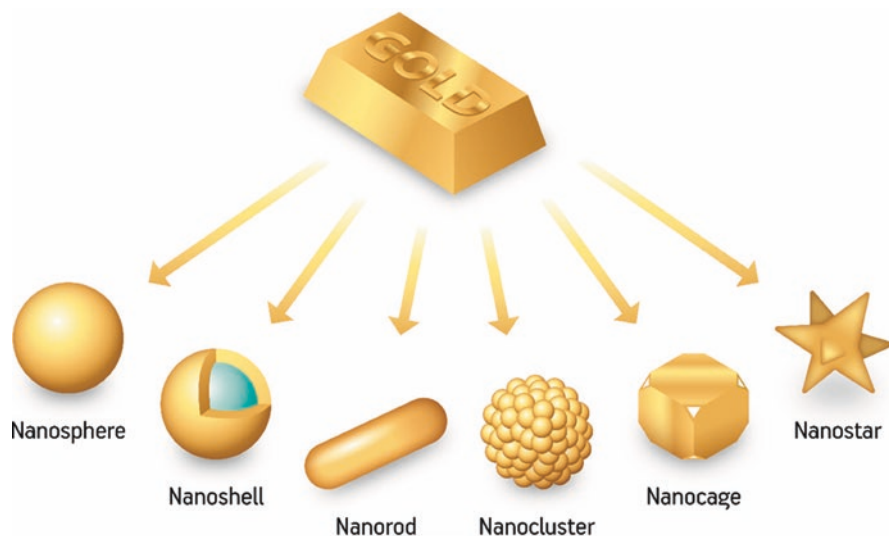


Fig. 9.1 Different types of AuNPs according to their shape and morphology. (Adapted from Freitas de Freitas et al. (2018))

nanospheres of reduced dispersity and defined size (i.e., 10 nm in diameter), was reported in 1993 (Giersig and Mulvaney 1993). The phase transfer reagent such as tetrabutylammonium bromide was used to improve this technique. Moreover, thiol/gold molar ratios can affect the average size of the nanospheres (Brust et al. 1994). Larger thiol-to-gold ratios and rapid addition of cold reductant solutions yield smaller and more monodispersed gold nanospheres. Many other methods have already been investigated for the synthesis of gold nanospheres using other reducing agents or ligands (Leff et al. 1996). On the other hand, dendrimers have been used as templates or stabilizers for the generation of Au nanospheres (Esumi et al. 1998). Biocompatible block copolymers have already been employed for the synthesis of sterically stabilized Au nanospheres in aqueous solution (Yuan et al. 2006). The shape and size of the Au nanospheres could be readily controlled by optimizing the synthesis parameters including block copolymer composition, relative/absolute concentrations of the block copolymer, and HAuCl_4 . It was also reported that Au nanospheres could be grown in human cells (Anshup et al. 2005). Furthermore, Au nanospheres display a single absorption peak in the visible range between 510 nm and 550 nm. The absorption peak shifts to a longer wavelength with the increasing particle size, and the width of the absorption spectra is related to the size distribution range. Many other types of AuNPs with different size/shape including nanorods, nanoshells, and nanocages have been explored to obtain optical properties suitable for biomedical applications.

9.2.2 *Au Nanorods*

The Au nanorods have received worldwide attention because of their inimitable shape-dependent optical properties (i.e., different plasmon bands) that make the Au nanorods exclusive materials for biological imaging, sensing, photothermal therapy, and drug delivery (Hainfeld et al. 2008; Kodiha et al. 2014; Nichols and Bae 2014; Choi et al. 2010). Their application is very precise because even a small change in the shape, size, and surface nature alter their properties which in turn affect their biological applications. The surface plasmon resonance (SPR) band of Au nanorods is in the NIR region that makes them suitable for photothermal therapy, biological sensing, and imaging (Martin 1994). The Au nanorods can be synthesized using the template method. The diameter of the template membrane pore can be used to determine the diameter of the Au nanorods, while the length of the nanorods can be controlled through the amount of gold deposited within the pores. The main disadvantage of this method is low yield since only one monolayer of nanorods is prepared. The formation of Au nanorods through electrochemical synthesis has been also reported (Reetz and Helbig 1994; Yu et al. 1997; Chang et al. 1999). According to this approach, many experimental parameters determine the length of the Au nanorods that influence their aspect ratio which is defined as the length divided by the width. On the other hand, the seed-mediated synthesis, the most established method for Au nanorod preparation, provides higher aspect ratio than that prepared by the other methods (Jana et al. 2001a; Busbee et al. 2003). Usually, Au seeds are prepared by chemical reduction of Au salt (i.e., $\text{HAuCl}_4 \cdot 3\text{H}_2\text{O}$) with a strong reducing agent including sodium borohydride (i.e., NaBH_4). These seeds, serving as the nucleation sites for Au nanorods, are then added to the growth solution containing Au salt, a weak reducing agent such as ascorbic acid, and hexadecyltrimethyl ammonium bromide. The aspect ratio of Au nanorods can be controlled by varying the amount of gold seeds with respect to the precursor. Furthermore, Au nanorods can be produced in quantitative yield upon addition of AgNO_3 (Jana et al. 2001b, 2002). Besides, several other types of approaches have also been investigated for the fabrication of Au nanorods including bioreduction (Canizal et al. 2001), growth on mica surface (Mieszawska and Zamborini 2005), and photochemical synthesis (Kim et al. 2006).

9.2.3 *Au Nanocages*

Gold (Au) nanocages are characterized by their ultrathin porous walls and hollow interiors. They are synthesized using silver nanoparticles (AgNPs) as template that participate in the galvanic replacement (GR) reaction (Skrabalak et al. 2007, 2008; Lu et al. 2007). The controllable pores on the surface of Au nanocages have been synthesized via galvanic replacement reaction between silver nanocubes and aqueous HAuCl_4 (Chen et al. 2006). The silver (Ag) nanostructures with controlled

morphologies can be generated through polyol reduction where AgNO_3 is reduced by ethylene glycol. Sequential addition of Ag atoms to the seeds produces the desired nanostructures by controlling Ag seed crystalline structures in the presence of poly(vinylpyrrolidone), a polymer capable of selectively binding to the surface. Ag nanostructures are used as supportive templates that can be transformed into Au nanostructures with hollow interiors via galvanic replacement (Chen et al. 2005, 2006). The wall thickness and dimension of the resultant Au nanocages could be readily controlled with high precision by adjusting the molar ratio of Ag to HAuCl_4 (Cai et al. 2008). The light penetration ability in soft tissues can be maximized by restricting the light source to near infrared (NIR) region (i.e., 650 to 900 nm). This is because the light absorption ability of hemoglobin and water is negligible in the NIR region. The LSPR peaks can be concisely tuned throughout the visible and NIR region to make the Au nanocages suitable for this application (Kwon et al. 2012; Mahmoud et al. 2010; Au et al. 2008; Mahmoud and El-Sayed 2010). Au nanocages can also be functionalized with the bioactive molecules to target cancer cells for diagnosis and photothermal therapy at an early stage (Dreaden et al. 2012; Chen et al. 2012).

9.2.4 Au Nanoshells

The Au nanoshells are composed of silica core coated by a thin Au metallic shell. The most interesting property of Au nanoshells is their unique surface plasmon resonance property that can be finely tuned from visible to NIR region. There are multiple templates employed for the formation of hollow Au nanoshells including silica particles (Averitt et al. 1997), metal particles (Oldenburg et al. 1998, Oldenburg et al. 1999a, b; Tuersun and Han 2013), and so on. The Au nanoshells have been applied in various biomedical applications such as whole-blood immunoassays and photothermal cancer therapy (Loo et al. 2005; Park et al. 2008; Bickford et al. 2010). Cancer cells were successfully ablated in vitro by Au nanoshells as observed through magnetic resonance thermal imaging. Furthermore, the use of Au nanoshells for the photothermal ablation of tumors in mice showed complete regression of tumors while the mice remain healthy (Gobin et al. 2007, 2008; Hirsch et al. 2003; Lowery et al. 2006). Optical imaging techniques including those that use AuNPs as the contrast agents have limited applications in human studies. On the other hand, in the NIR region (i.e., 700–900 nm), the absorbance of all the bioactive molecules is negligible which provides clear window for optical imaging (Frangioni 2003). Au nanoshells can be designed and fabricated to control the location of surface plasmon resonance (SPR) peaks from visible to the NIR region of the electromagnetic spectrum by varying the composition and dimensions of the layers (Oldenburg et al. 1999a). The SPR peak can also be tuned by changing the ratio of the core size to its shell thickness for a given composition of Au nanoshells. Furthermore, Au nanoshells with SPR peaks in the NIR region can be prepared by coating Au shells with silica or polymer beads of variable thickness (Oldenburg et al. 1998; Caruso

et al. 2001). The silica cores are grown according to the Stöber process, that is, the reduction of tetraethyl orthosilicate in basic ethanol. A seed-mediated growth technique is typically used to coat the silica nanoparticles with Au in an aqueous environment. The small Au nanospheres, such as 2–4 nm in diameter, can be attached to the silica core using an amine-terminated silane as a linear molecule that allows additional Au to be reduced until the seed particles coalesced into a complete shell (Oldenburg et al. 1999b). The diameter of the gold nanoshells is mainly determined by the diameter of the silica core, and the shell thickness can be controlled through the amount of gold deposited on the surface of the core. Gold nanoshells have also been synthesized via in situ gold nanoparticle formation using thermosensitive core-shell particles as the template (Suzuki and Kawaguchi 2005). The use of different microgels as the core offers significantly reduced particle aggregation. The thickness of Au nanoshells was also controlled through electroless deposition of Au. Recently, a virus scaffold has been used to assemble Au nanoshells which may potentially provide cores with a narrower size distribution and smaller diameters (i.e., 80 nm) than that of silica (Radloff et al. 2005).

9.2.5 Au Nanostars

Gold (Au) nanostars belong to the anisotropic AuNPs category. Au nanostars are composed of a core and several branches with sharp tips. The unique characteristics of Au nanostars originate from these branches and their interaction with the core. The attractive features of Au nanostars are localized surface plasmon resonance (LSPR), surface-enhance Raman Scattering (SERS) activity, and catalytic activity. The Au nanostars are used for catalysis, nanosensing assays, thermal therapy, and drug delivery. The Au nanostars have multiple sharp branches that demonstrate significant electromagnetic field enhancement and have unique plasmon bands which can be tuned from visible to NIR region. The synthesis of Au nanostars has been driven by the interest on the localized surface plasmons (LSPs) response to the environment, especially on sharp tips and edges, where light can be highly concentrated (Hao et al. 2007; Rodríguez-Lorenzo et al. 2009; Hrelescu et al. 2009; Dondapati et al. 2010). They serve as effective tools in the field of nanomedicine due to their unique properties. The Au nanostars also display stronger surface-enhanced resonance activity than Au spheres or even rods (Mukherjee et al. 2001; Cai et al. 2008).

9.3 Antibacterial Activity of AuNPs

Although gold nanoparticles (AuNPs) are not strong antimicrobial agent as AgNPs, they have been reported to demonstrate antibacterial (Lima et al. 2013) as well as antifungal activity (Wani and Ahmad 2013; Zawrah et al. 2011). Furthermore,

AuNPs have been used as an alternative tool to high-dose antibiotics against infectious diseases including antibiotic-resistant bacteria (Podsiadlo et al. 2008). The nanoparticle toxicity and antibacterial activity mainly depend on the intrinsic properties, surface modification, and tested bacterial species. The AuNPs of smaller diameter can penetrate the bacterial cells and cause cellular damage followed by death (Bindhu and Umadevi 2014a). Antibacterial properties of triangular-shaped AuNPs demonstrate better activity toward both gram-positive and gram-negative bacteria than that of spherical AuNPs (Smitha and Gopchandran 2013). The sharp-faced triangular NPs, irrespective of their surface chemistry, size, and composition, can pierce the endosomal membrane before translocating to the cytoplasm where they can be retained. This feature makes them preferable to round-shaped NPs for drug delivery, gene delivery, subcellular targeting, and long-term tracking (Chu et al. 2014). Recently, it has been reported that very small AuNPs (i.e., less than 2 nm) showed excellent antibacterial activity against gram-positive and gram-negative bacteria (Kundu 2017).

9.3.1 Antibacterial Activity Against Pathogenic Bacteria

The AuNPs synthesized using citrate, polyvinylpyrrolidone (PVP), or other commonly used stabilizers usually do not show antibacterial activity (Amin et al. 2009). More specifically, the AuNPs (size: 20–30 nm) stabilized by PVP and/or sodium dodecyl sulfate (SDS) did not show antimicrobial activity against *Staphylococcus aureus* ATCC 6538, *Escherichia coli* K12 NCTC 10538, and fungi *Candida albicans* ATCC 10231 at a concentration of 0.0016 wt% (Mukha et al. 2010). Chatterjee et al. (2011) found that AuNPs showed no concentration-dependent antibacterial activity while stimulating the level of cell division. AuNPs are biologically inert and usually do not show antibacterial activity (Allahverdiyev et al. 2011) that can be convinced from their high MIC value and small zone of inhibition (ZOI) value when compared to AgNPs. Hernández-Sierra et al. (2008) compared the antibacterial activity of AgNPs (size: 25 nm) with that of AuNPs (size: 80 nm) against *S. aureus* ATCC 25923. The AgNPs had a MIC (minimum inhibitory concentration) value of 4.86 ± 2.71 $\mu\text{g/ml}$ and MBC (minimum bactericidal concentration) value of 6.25 $\mu\text{g/ml}$. On the other hand, AuNPs showed antibacterial propensity at a very high concentration (197 $\mu\text{g/ml}$). Shankar et al. (2014) synthesized AuNPs, AgNPs, and Au-AgNPs having hydrodynamic size 140 ± 13 , 74 ± 6 , and 128 ± 15 nm, respectively. The growth of *S. aureus* and *E. coli* was inhibited at 16 $\mu\text{g/ml}$ and 8 $\mu\text{g/ml}$ of AgNPs, respectively. Similar pattern of inhibition was also observed for Au-AgNPs having MIC value 16 and 32 $\mu\text{g/ml}$ against *S. aureus* and *E. coli*, respectively. On the other hand, AuNPs did not show any antibacterial activity at the tested concentration (i.e., 128 $\mu\text{g/ml}$). Sreelakshmi et al. (2011) compared the antibacterial activity of AuNPs and AgNPs (size: 10 nm) synthesized using natural honey as a source of stabilizing as well as reducing agent. Their MIC values confirmed that honey-capped AgNPs exhibit very good antibacterial activity, whereas AuNPs exhibit

moderate activity against the tested strains. On the other hand, PVP-coated AuNPs have ~10 times higher MIC value than that of AgNPs synthesized using the same polymer (Mukha et al. 2010; Hernández-Sierra et al. 2008). Hence, AuNPs are not usually used as antibacterial agents. In addition, incorporation of AuNPs (2 nm), methylene blue (MB), and toluidine blue (TBO) with polyurethane polymer, a polymer used to prepare catheters, enhanced the killing of *S. aureus* suspension under white illumination with a hospital light source (Naik et al. 2011). However, many other studies have revealed that AuNPs synthesized under certain conditions showed efficient antibacterial activity and they can be functionalized with different biopolymers to make an effective antibacterial agent. The size, shape, surface modification (coating and capping agents), and purification methods of AuNPs are the key factors that determine their antibacterial activity. However, CTAB-coated AuNPs of 1~2 nm and 1~20 nm in size were reported to show similar zone of inhibition (~22 mm) against *E. coli* (ATCC 25922 strain) without any size dependence (Azam et al. 2009; Arshi et al. 2011).

Furthermore, Badwaik et al. (2012) investigated the antibacterial activity of dextrose-coated AuNPs having different hydrodynamic diameters such as 25, 60, and 120 ± 5 nm. AuNPs with hydrodynamic diameter of 120 and 60 nm inhibit the proliferation of *E. coli* in a concentration-dependent manner and the MIC values were 16×10^{10} and 16×10^{11} particles/ml, respectively. On the other hand, AuNPs having 25 nm hydrodynamic diameter did not show any significant effect against the proliferation of *E. coli* even at concentration as high as 128×10^{12} particles/ml. Hence, they concluded that the antibacterial activity of AuNPs increases as the particle size increases, for example, in the order of $25 < 60 < 120 < \text{nm}$. On the other hand, Ahmad et al. reported that smaller AuNPs (i.e., 7 nm) showed excellent antifungal activity and greater biocidal effect against *Candida* species when compared to that of relatively large AuNPs (i.e., 15 nm) (Ahmad et al. 2013). The capping agent is also an important determinant of the antibacterial activity of AuNPs. Zhang et al. (2008) synthesized hyperbranched poly(amidoamine) having terminal dimethylamine groups (HPAMAM-N $(\text{CH}_3)_2$) to prepare AuNPs and they found that the cationic dimethylamine contributes to the antimicrobial activity through strong ionic interactions with bacteria. As shown in Table 9.1, AuNPs stabilized or modified by various coating agents have distinct antibacterial effects. Many small molecules were also used for the synthesis of AuNPs and were investigated for their antibacterial potential. For example, 4, 6-diamino-2-pyrimidinethiol (DAPT), an analogue of 2-pyrimidinethiol that is present in *E. coli*; two positively charged and amino-substituted pyrimidines 4-amino-2-pyrimidinethiol and 2,4-diamino-6-pyrimidine thiol (iDAPT) (Chatterjee et al. 2011); and one negatively charged pyrimidine 4,6-dihydroxyl-2-pyrimidine thiol (DHPT) (Zhao et al. 2010) were used to fabricate AuNPs. The MIC values of DAPT, APT, and iDAPT fabricated AuNPs against *Pseudomonas aeruginosa* were 16, 18, and 24 $\mu\text{g/ml}$, respectively. DHPT-coated AuNPs did not inhibit the growth of both *E. coli* and *P. aeruginosa* even at high concentration (80 $\mu\text{g/ml}$).

The methods used for the purification of AuNPs were neither mentioned nor adequately carried out before performing antibacterial assay. There could be debate

Table 9.1 A summary of the antibacterial activity of AuNPs synthesized using different types of reducing agents and capping agents

AuNPs (reducing agents and capping agents)	Size (if present)	Test bacteria	Effect of antibacterial activity	Ref.
Citric acid Polyallylamine HCl	20–30 nm	<i>B. Calmette-Guérin</i> <i>E. coli</i>	Effect and mechanism depend upon composition and surface modifications	Zhou et al. (2012)
Citrate/CTAB	1–22 nm	<i>E. coli</i>	AuNPs show high antibacterial activity with zone of inhibition of 22 mm	Zhang et al. (2015)
Acridine derivatives	15–20 nm	<i>E. coli</i> <i>Bacillus subtilis</i>	Acridine-AuNPs has stronger antibacterial effect than acridine alone	Mitra et al. (2014)
Citrate	20–30 nm	<i>E. coli</i>	Dose-dependent inhibition, 0.1–5 µg/mL	Zhou et al. (2012)
Phosphine	–	<i>S. aureus</i>	Antibacterial activity of two ligands are compared	Borah et al. (2011)
Pyrimidine thiols	3 nm	<i>P. aeruginosa</i>	MICs of Au-DAPT, Au-APT, and Au-iDAPT are 16, 18, and 24 µg/mL	Zhao et al. (2010)
Thioguanine	–	<i>Micrococcus luteus</i> <i>S. aureus</i> <i>P. aeruginosa</i> <i>E. coli</i>	AuNPs are more potent than thioguanine	Selvaraj et al. (2010)
PVP/SDS	20–30 nm	<i>S. aureus</i> <i>E. coli</i> K12	AuNP of 0.0016% wt. showed no effect on tested strains	Mukha et al. (2010)
Gallic acid	14, 39, 77 nm	<i>S. mutans</i>	MICs of 12.31, 12.31, and 49.25 µg/mL for 13.7, 39.4, and 76.7 nm AuNPs	Moreno-Álvarez et al. (2010)
Reduced by lysozyme at 40 °C	–	<i>Acinetobacter baumannii</i> <i>Enterococcus faecalis</i>	Broad-band labeling agents for pathogenic bacteria	Chen et al. (2010)
Citrate, CTAB	1 ~ 22 nm	<i>E. coli</i>	Zone of inhibition of 22 mm	Arshi et al. (2011), Zhang et al. (2015)
Polyamidoamine	7.7, 4.6, 3.9 nm	<i>E. coli</i> <i>S. aureus</i> <i>B. subtilis</i> <i>Klebsiella mobilis</i>	Inhibit up to AuNP (2.8 µg/mL) Ionic interaction with bacteria	Zhang et al. (2008)
PVP	80 nm	<i>S. aureus</i>	MIC, > 197 µg/mL	Hernández-Sierra et al. (2008)

(continued)

Table 9.1 (continued)

AuNPs (reducing agents and capping agents)	Size (if present)	Test bacteria	Effect of antibacterial activity	Ref.
Polythiophene composite	–	Common bacterial pathogens	Efficient antibacterial effect was observed	Adhikari et al. (2013)
Citrate or PAH	2–30 nm	<i>E. coli</i>	<i>E. coli</i> growth inhibited at 0.1, 1, 5 µg/mL citrate-AuNPs	Zhou et al. (2012)
Capped by amine or polyacrylate	–	<i>E. coli</i>	99.999% killing in 10 min. Coating agents are responsible for antibacterial activity	Wan and Yeow (2012)
Dextrose	25, 60, and 120 nm	<i>E. coli</i>	For 120 and 60 nm AuNPs with MIC 16×1010 and 16×1011 NPs/mL for 25 nm AuNPs, no inhibition at 128×1012 NPs/mL	Badwaik et al. (2012)
Cationic peptides	1.2–2.5 nm	<i>S. aureus</i> <i>B. subtilis</i> <i>E. coli</i> <i>P. aeruginosa</i>	MIC higher with AuNP than without	Pal et al. (2011)
Zeolite (2.3–2.8%)	5 nm	<i>E. coli</i> <i>Salmonella typhi</i>	Eliminate 90–95% of <i>E. coli</i> and <i>S. typhi</i> colonies at short time	Lima et al. (2013)
Polyoxometalates and lysine	–	<i>E. coli</i>	5 µM causes 80% bacterial death	Daima et al. (2013)
Cationic monolayer	2 nm	MDR strains and MRSA	MIC values dependent on side chain functional groups and chain length	Li et al. (2014)
Zeolite	–	<i>E. coli</i> <i>S. Typhi</i>	AuNPs dispersed on zeolites eliminate <i>E. coli</i> and <i>S. typhi</i> at short times	Zhang et al. (2015)

on the antibacterial activity of AuNPs because of the presence of capping agents or other reagents used for the synthesis of nanoparticles that were not purified properly. It might be, therefore, the presence of Au(III) ions as well as unreacted reagents interfere with the antibacterial results, thereby producing false results. Several studies have reported the purification of chemically synthesized AuNPs prior to investigating their antimicrobial activity. For example, Daima et al. synthesized tyrosine-functionalized AuNPs and dialyzed to remove free ions and unbound tyrosine prior to investigating their antibacterial activity to avoid any interference on their toxicity bacteria (Daima et al. 2013). Furthermore, Zhou et al. (2012) prepared citrate-stabilized AuNPs followed by purification through centrifugation to test antibacterial activity against *E. coli* and *Bacillus Calmette-Guérin*. Nazari et al. also reported the synthesis and purification of AuNPs before testing their antibacterial activity against *P. aeruginosa*, *S. aureus*, and *E. coli* (Nazari et al. 2012).

On the other hand, AuNPs were also synthesized and fabricated using natural polymers extracted from either microorganisms or plants, or directly in the presence of microorganisms. They are summarized in Table 9.2. These processes are known as green or eco-friendly synthesis or biosynthesis. For instance, Nagaraj et al. (2012) synthesized spherical AuNPs (size: 10–50 nm) using *Caesalpinia pulcherrima* flower extract as the reducing agent that showed efficient antimicrobial activity against *Aspergillus*, *E. coli*, and *Streptobacillus* sp. Das et al. (2009) synthesized AuNPs (size: 10 nm) on the surface of *Rhizopus oryzae* MTCC 262 through in situ reduction of HAuCl_4 that showed high antibacterial activity against several gram-positive and gram-negative pathogenic bacteria. Mishra et al. (2011) synthesized AuNPs (size: 50–70 nm) and AgNPs (size: 10–20 nm) via extracellular synthesis using yeast *Candida guilliermondii* and the highest antibacterial activity for both AuNPs and AgNPs was found against *Staphylococcus aureus*. AuNPs were also synthesized using various plant extracts including *Mentha piperita* (MubarakAli et al. 2011), root extract of *Trianthema decandra*, (33–65 nm) (Geethalakshmi and Sarada 2012), *Helianthus annuus* flower extracts (Geethalakshmi and Sarada 2012), and dried flower extract of *Carthamus tinctorius* (Liny et al. 2012). Interestingly, all the green synthesized AuNPs demonstrated efficient antibacterial activity against several bacteria strains that were unaffected in the presence of chemically synthesized AuNPs (Mishra et al. 2011). Finally, the question is what is responsible for the antibacterial activity of green-synthesized AuNPs. It may be due to the extracts alone, AuNPs or their combination with plant extracts, since several plant extracts including *Euphorbia hirta* plant alone demonstrated antibacterial activity (Annamalai et al. 2013). Hence, the antibacterial activity may also be due to the synergistic effect of the combination of AuNPs and extracts (Annamalai et al. 2013).

9.3.2 Antibacterial Activity Against Multidrug-Resistant (MDR) Bacteria

Metallic gold is inert and non-toxic that may change when shifts from metallic to oxidation states (0, I, and III) (Merchant 1998). The antibacterial mechanism of AuNPs is associated with (i) the collapse of membrane potential that inhibits the ATPase activity and causes deterioration of the cellular metabolism and (ii) inhibition of the binding subunit of ribosomes to tRNA (Cui et al. 2012). Also (iii) Shamaila and co-workers showed that AuNPs disrupt the bacterial respiratory chain by binding to the thiol group of enzymes including nicotinamide adenine (NADH) dehydrogenase and produce oxidative stress resulting in the cellular death (Shamaila et al. 2016). Since AuNPs are non-toxic to the host (Li et al. 2014; Conde et al. 2014; Rajchakit and Sarojini 2017), the possibility of fine-tuning their conjugation ability to act as carriers of antibiotics or other antibacterial moieties may enhance their bactericidal effect as well as potentiate the effect of antibiotics (Baptista et al. 2018). Functionalization of AuNPs with cationic and hydrophobic polymers was

Table 9.2 A summary of antibacterial activity of AuNPs synthesized using “green” method

AuNPs (green method)	Size (if present)	Test bacteria	Effect of antibacterial activity	Ref.
Black tea extract	2–100 nm	<i>P. aeruginosa</i> <i>S. aureus</i> <i>E. coli</i>	AuNPs did not increase antibacterial activity at concentration of 40 µg/disc	Nazari et al. (2012)
<i>Shewanella oneidensis</i>	12 ± 5 nm	<i>E. coli</i> <i>S. oneidensis</i> <i>B. subtilis</i>	No bactericidal effect for the tested strains at concentrations of 150 µM	Suresh et al. (2011)
<i>Punica Granatum</i>	5–17 nm	<i>S. aureus</i> <i>S. typhi</i> <i>Vibrio cholerae</i>	MIC values for the tested bacteria – 0.33, 0.37 and 0.41 mg/mL	
<i>C. zeylanicum</i> leaf broth	>100 nm	<i>E. coli</i> <i>S. aureus</i>	Efficient antibacterial activity	Smitha and Gopchandran (2013)
<i>Memecylon umbellatum</i> leaf	15–25 nm	<i>B. subtilis</i> <i>E. coli</i> <i>S. pneumoniae</i> <i>S. aureus</i> <i>S. typhimurium</i> <i>K. aerogenes</i>	Inhibited bacterial growth	Arunachalam et al. (2013)
<i>E. hirta</i>	6–71 nm	<i>E. coli</i> <i>P. aeruginosa</i> <i>K. pneumoniae</i>	Complete inhibition at a concentration of 200 µg/mL	Annamalai et al. (2013)
<i>T. decandra</i>	33–65 nm	<i>P. vulgaris</i> <i>E. coli</i> <i>S. aureus</i> <i>S. faecalis</i>	Excellent activity at a concentration of 10 mg/L on each disc	Geethalakshmi and Sarada (2012)
<i>Solanum nigrum</i>	18–20 nm	<i>B. subtilis</i> <i>E. coli</i> <i>P. aeruginosa</i>	Inhibited bacteria growth	Balagurunathan et al. (2011)
<i>Phyllanthus emblica</i>	2–4 nm	<i>S. aureus</i> <i>E. coli</i>	Zone of inhibition, 0.8–1.0 cm	Balasubramanian (2014)
<i>Gracilaria corticata</i>	45–57 nm	<i>S. aureus</i> <i>E. faecalis</i> <i>E. coli</i> <i>Enterobacter aerogenes</i>	Antimicrobial activity observed for tested bacteria at 24, 21, 19 and 14 mm	Naveena and Prakash (2013)
Phytochemicals	15–35 nm	<i>E. coli</i> <i>B. subtilis</i> <i>S. aureus</i> <i>Enterococci</i>	AuNPs showed zone of inhibition against all the studied bacteria	Mahitha et al. (2013)
Soybean Polyphenols	7–12 nm	<i>S. aureus</i> <i>P. aeruginosa</i> <i>A. baumannii</i>	Gram-negative bacteria with thin cell wall were more susceptible to cell wall damage compared to gram-positive bacteria	El-Batal et al. (2013)

(continued)

Table 9.2 (continued)

AuNPs (green method)	Size (if present)	Test bacteria	Effect of antibacterial activity	Ref.
<i>Rhizopus oryzae</i> MTCC 262	10 nm	<i>P. aeruginosa</i> <i>E. coli</i> <i>B. subtilis</i> <i>S. aureus</i>	Inhibition starts at 50 µg/mL caused rupture of cell membrane	Das et al. (2009)
<i>Saururus chinensis</i> leaf	–	<i>S. aureus</i> <i>E. coli</i>	27.6% inhibition with AuNPs of 0.2 mM and >90% inhibition after 24 h exposure at AuNPs of 0.8–1 µM	Sreekanth et al. (2012)
Reduced by <i>C. tinctorius</i> flower	–	<i>S. aureus</i> <i>E. coli</i> <i>B. subtilis</i>	Efficient antibacterial effect was observed	Nagajyothi et al. (2012)
Treatment with root extract of <i>T. decandra</i>	33–65 nm	<i>E. faecalis</i> <i>S. aureus</i> <i>S. faecalis</i> <i>B. subtilis</i> <i>Y. enterocolitica</i> <i>P. vulgaris</i> <i>E. coli</i> <i>P. aeruginosa</i>	Inhibition areas (mm) for <i>E. faecalis</i> 10.5, <i>S. aureus</i> 14.5, <i>S. faecalis</i> 13.5, <i>B. subtilis</i> 9.5, <i>Y. enterocolitica</i> 15.5, <i>P. vulgaris</i> 15.0, <i>E. coli</i> 9.5, <i>P. aeruginosa</i> 11.5	Geethalakshmi and Sarada (2012)
<i>Ananas comosus</i>	–	<i>E. coli</i> <i>Streptobacillus sp</i>	Effective on <i>E. coli</i> & <i>Streptobacillus sp</i>	Basavegowda et al. (2013)
<i>Euphorbia hirta</i>	6–71 nm	<i>E. coli</i> <i>P. aeruginosa</i> , <i>K. pneumoniae</i>	Inhibited 88% <i>E. coli</i> , 86% <i>P. aeruginosa</i> , and 94% <i>K. pneumoniae</i> at 200 µg/mL; plant <i>E. hirta</i> has antibacterial activity itself	Annamalai et al. (2013)
<i>Solanum torvum</i>	–	<i>E. coli</i> <i>Pseudomonas</i> <i>Bacillus</i>	AuNPs showed strong and fair zone of inhibition	Ramamurthy et al. (2013)
<i>Dioscorea batatas</i>	18–56 nm	Gram-positive and gram-negative bacteria	AuNPs inhibited <i>S. aureus</i> , <i>S. epidermidis</i> , <i>E. coli</i> ; 21.5% inhibition by 0.2 µM and >50% by 0.8–1 µM AuNPs	Sreekanth et al. (2015)
LD fruit peel	140, 74, 128 nm	<i>S. aureus</i> <i>E. coli</i>	No antibacterial activity at >128 µg/mL for AuNPs, but for AgNPs and Au-Ag-NPs	Shankar et al. (2014)

(continued)

Table 9.2 (continued)

AuNPs (green method)	Size (if present)	Test bacteria	Effect of antibacterial activity	Ref.
<i>Abelmoschus esculentus</i>	14 nm	<i>B. subtilis</i> <i>B. cereus</i> <i>P. aeruginosa</i> <i>M. luteus</i> <i>E. coli</i>	AuNPs (0.2 mg/mL) showed inhibition zones of 26, 24, 15, 35 and 21 mm against <i>B. subtilis</i> , <i>B. cereus</i> , <i>E. coli</i> , <i>M. luteus</i> , <i>P. aeruginosa</i>	Mollick et al. (2014)
<i>Trichoderma viride</i> , <i>Hypocrea lixii</i>	61 nm	<i>E. coli</i> <i>Shigella sonnei</i> <i>P. syringae</i>	Inhibition of the growth of <i>E. coli</i> , <i>S. sonnei</i> , and <i>P. syringae</i> up to 53%, 47%, 55%	Mishra et al. (2014)
<i>Punica granatum</i>	5 and 20 nm	<i>S. aureus</i> <i>S. typhi</i> <i>V. cholerae</i>	MICs against <i>S. aureus</i> , <i>S. typhi</i> , <i>V. cholerae</i> are 0.33, 0.37, 0.41 mg/mL	Lokina et al. (2014)
<i>Solanum lycopersicum</i>	14 nm	<i>S. aureus</i> <i>P. aeruginosa</i>	Effective inhibition of growth of all tested bacteria	Bindhu and Umadevi (2014b)
<i>Mentha piperita</i>	150 nm	<i>E. coli</i> <i>S. aureus</i>	Effective against <i>aureus</i> <i>E. coli</i> , but not <i>S. aureus</i>	MubarakAli et al. (2011)
<i>Candida guilliermondii</i>	50–70 nm	Five pathogenic bacterial strains	Highest inhibition against <i>S. aureus</i> ; chemically synthesized AuNPs showed no effect	Mishra et al. (2011)
<i>Trianthema decandra</i> or saponin	37.7–79.9 nm	10 different bacteria	Zones of inhibition of 8.2 mm to 11.5 mm; excellent activity against <i>Y. enterocolitica</i> , <i>P. vulgaris</i> , <i>E. coli</i> , <i>S. aureus</i> , <i>S. faecalis</i>	Geethalakshmi and Sarada (2013)
Grapes fruit	–	<i>P. aureus</i> <i>S. typhi</i> <i>V. cholerae</i>	Excellent antibacterial activity toward most of the tested bacterial strains	Lokina et al. (2014)

shown to be effective against both gram-negative and gram-positive uropathogens including MRSA. These AuNPs exhibited low toxicity to mammalian cells, and development of resistance to these nanoparticles was very low (Li et al. 2014). Vinoj et al. demonstrated that the conjugation of AuNPs with N-acylated homoserine lactonase proteins (AiiA AuNPs) resulted in a nano-composite with greater antibacterial activity against MDR species when compared to AiiA proteins alone (Vinoj et al. 2015).

The integration of AuNPs on the shell of PVA-lysozyme microbubbles demonstrated better antibacterial potential against *E. coil* than that of only microbubbles (Mahalingam et al. 2015). Galic acid-capped AuNPs have also been found to be active against gram-negative and gram-positive bacteria (Kim et al. 2017). Recently, Ramasamy et al. reported one-pot synthesis of cinnamaldehyde-immobilized gold

nanoparticles (CGNPs) having more than 80% effectivity against biofilm formation of gram-positive (methicillin-sensitive and -resistant strains of *S. aureus*, MSSA, and MRSA, respectively) and gram-negative (*E. coli* and *P. aeruginosa*) bacteria (Ramasamy et al. 2017a, b). The incorporation of AuNPs with ultrathin graphitic carbon nitride ($g\text{-C}_3\text{N}_4$) generates peroxidase activity and demonstrates excellent antibacterial potential against drug-resistant (DR) gram-positive and gram-negative bacteria. They also exhibit high efficiency in eliminating existing DR biofilms and preventing the formation of new biofilms in vitro (Wang et al. 2017a). The conjugation of antibiotics (e.g., vancomycin and methicillin) to AuNPs increases their intrinsic activity against MDR strains (Baptista et al. 2018). Recently, Payne et al. developed a single-step synthesis technique for kanamycin-capped AuNPs (Kan-AuNPs) that exhibit high antibacterial activity against both gram-positive and -negative bacteria including kanamycin-resistant bacteria. The authors observed a significant reduction in the MIC value against all the bacterial strains tested when compared to free drug. This higher efficacy was due to the disruption of the bacterial envelope that resulted in the leakage of cytoplasmic content and thereby cell death (Payne et al. 2016). Pradeepa et al. synthesized AuNPs using bacterial exopolysaccharide (EPS) and functionalized them with antibiotics (e.g., levofloxacin, cefotaxime, ceftriaxone, and ciprofloxacin). They observed that antibiotic-conjugated AuNPs exhibited excellent bactericidal activity against MDR gram-positive and -negative bacteria when compared to free drugs. *E. coli* was the most susceptible MDR bacteria followed by *K. pneumoniae* and *S. aureus* (Vidya et al. 2016). Recently, Yang et al. described the effect of small molecule (6-aminopenicillanic acid, APA) coated AuNPs to inhibit MDR bacteria (Yang et al. 2017). They conjugated AuNPs with electrospun fibers of poly(ϵ -caprolactone) (PCL)/gelatin to produce materials that inhibit wound infection by MDR bacteria and also demonstrated that APA-AuNPs reduce MDR bacterial infections (Yang et al. 2017). Shaker et al. evaluated the surface functionalization of AuNPs with carbapenems [i.e., imipenem (Ipm) and meropenem (Mem)] and investigated their antibacterial activity against carbapenem-resistant gram-negative bacteria isolated from an infected human. Both Ipm-AuNPs and Mem-AuNPs (size: 35 nm) showed significant increase in their antibacterial activity against all the tested isolates (Shaker and Shaaban 2017). Recently, Shaikh et al. described the synthesis and characterization of cefotaxime-conjugated AuNPs to target drug-resistant CTX-M-producing bacteria. The authors inverted resistance in cefotaxime-resistant bacterial strains (i.e., *E. coli* and *K. pneumoniae*) by using cefotaxime-AuNPs. Hence, the conjugation of unresponsive antibiotics with AuNPs can restore their antibacterial activity against drug-resistant bacterial strains (Shaikh et al. 2017).

One of the most important properties of AuNPs is their ability to generate heat upon illumination with laser (Mendes et al. 2017; Mocan et al. 2017). This property is very important because it can be exploited to develop photothermal nano-vectors to destroy MDR bacteria at the molecular level (Mocan et al. 2017). For example, Khan et al. showed that the combination of Concanavalin-A (ConA)-directed dextran capped AuNPs ($\text{GNP}_{\text{DEX-ConA}}$) conjugated with methylene blue (MB) ($\text{MB@GNP}_{\text{DEX-ConA}}$)-mediated photodynamic therapy (PDT) enhanced the efficacy and

selectivity of MB-induced killing of MDR clinical isolates including *E. coli*, *K. pneumoniae*, and *Enterobacter cloacae* (Khan et al. 2017). Gil-Tomas et al. reported that the covalent conjugation of AuNPs with toluidine blue O–tiopronin forms an enhanced and exceptionally potent antimicrobial agent when activated by white light or 632 nm laser light (Gil-Tomás et al. 2007).

Hu et al. modified the surface of AuNPs with pH-responsive mixed charged zwitterionic self-assembled monolayers composed of weak electrolytic 11-mercaptoundecanoic acid (HS-C10-COOH) and strong electrolytic (10-mercapto-decyl) trimethylammonium bromide (HS-C10-N4) that exhibited an enhanced photothermal ablation of MRSA biofilm without any damage to the healthy tissues around the biofilm when illuminated with near infrared (NIR) laser (Hu et al. 2017). Furthermore, the antibacterial activity of glucosamine-gold nanoparticle-graphene oxide (GlcN-AuNP-GO) and UV-irradiated GlcN-AuNP-GO was evaluated against *E. coli* and *E. faecalis*. UV irradiation of GlcN-AuNP-GO demonstrated higher antibacterial activity than antibiotic kanamycin (Govindaraju et al. 2016).

Ocsoy et al. developed DNA aptamer-functionalized AuNPs (Apt@AuNPs) and gold nanorods (Apt@AuNRs) to kill methicillin-resistant *Staphylococcus aureus* (MRSA) through photothermal therapy (PTT) (Ocsoy et al. 2017). They found that both Apt@AuNPs and Apt@AuNRs attached to MRSA and inactivated cells by 5% and > 95%, respectively, through PTT. The difference in the induction of cell death was based on the relatively high longitudinal absorption of NIR radiation and strong photothermal conversion capability of the Apt@AuNRs compared to Apt@AuNPs. Recently, a new approach based on the conjugation of AuNPs with antimicrobial peptides (AMPs) has shown promising results (Rajchakit and Sarojini 2017). For example, Kuo et al. mixed synthetic peptides containing arginine, tryptophan, and cysteine termini [i.e., (DVFLG) 2REEW4C and (DVFLG) 2REEW2C] with aqueous tetrachloroauric acid to generate peptide-immobilized AuNPs [i.e., (DVFLG) 2REEW4C-AuNPs and (DVFLG) 2REEW2C-AuNPs] that were effective against *Staphylococci*, *Enterococci*, and other antibiotic-resistant bacterial strains (Kuo et al. 2016). Conjugation of AMPs with AuNPs usually involves the formation of Au-S coordinate covalent bond between the amine and thiol groups of peptides or conjugating linkers as well as terminal (N- or C-terminal) cysteine of AMPs which help in their conjugation with gold (Tielens and Santos 2010; Xue et al. 2014). However, there is one example when covalent conjugation of an AMP to AuNPs has been achieved via Au-O bond (Lai et al. 2015). Other approaches used a polyethylene glycol linker to covalently attach AMPs with AuNPs that showed significantly increased antibacterial and anti-biofilm activity against antibiotic-resistant gram-negative bacteria (Casciaro et al. 2017). Yeom and co-workers demonstrated the most advanced clinical application for AuNPs@AMP using infected mice in vivo that resulted in the inhibition of *Salmonella typhi* colonization in the organs of the animals (Yeom et al. 2016). The reason behind the increased antimicrobial activity of AuNPs@AMP over the free AMPs is that AuNPs can get a higher concentration of the peptides at the site of action. These NPs interact with lipopolysaccharides (LPS) and proteins of bacterial membrane and, in some cases, penetrate the

bacterial membrane through the porin channel. Thus, the nanoparticles interact with the bacterial inner membrane making the AuNPs@AMP conjugate more efficient than the non-conjugated form (Baptista et al. 2018). Rai et al. demonstrated the conjugation of cecropin-melittin (CM-SH), a known peptide with inherent antibacterial propensity (Boman et al. 1989), with the surface of AuNPs through Au-S bond. The CM-SH-AuNPs showed greater antimicrobial activity in a systemic (i.e., animal) model than CM-SH (Rai et al. 2016) (Table 9.3).

Table 9.3 Mechanism of antibacterial activity of AuNPs against multidrug-resistant (MDR) bacteria

Type of antibiotic resistance	Targeted bacteria	Mechanisms of antibacterial activity of AuNPs	Ref.
Methicillin resistant	<i>S. aureus</i>	Photothermal therapy with ROS generation	Hu et al. (2017), Ocsoy et al. (2017), Kuo et al. (2009), Millenbaugh et al. (2015), Mocan et al. (2016)
Methicillin resistant	<i>E. faecalis</i>	Combination with vancomycin	Lai et al. (2015)
Ampicillin resistant	<i>S. aureus</i> , <i>E. coli</i> , <i>P. aeruginosa</i> , <i>Enterobacter aerogenes</i>	Combination with ampicillin lead to entry into the bacterial cell	Brown et al. (2012)
Carbapenems resistant	<i>Klebsiella pneumoniae</i> , <i>Proteus mirabilis</i> , <i>A. baumannii</i>	Disturbance of osmotic balance and disruption of the integrity of bacterial cell wall	Shaker and Shaaban (2017)
Cefotaxime resistant	<i>E. coli</i> , <i>K. pneumoniae</i>	Disruption of the bacterial cell wall, DNA damage	Shaikh et al. (2017)
Kanamycin-resistant	<i>Streptococcus bovis</i> , <i>S. epidermidis</i> , <i>E. aerogenes</i>	Disruption of the bacterial cell wall	Payne et al. (2016)
Biofilm formation	<i>P. aeruginosa</i>	Interaction with cell surface	Yu et al. (2016)
Biofilm formation	<i>S. aureus</i>	Laser excitation of the near IR LSPR led to an efficient photothermal response with efficient killing of bacteria biofilms	Pallavicini et al. (2014)
Biofilm formation	<i>S. epidermidis</i> , <i>S. haemolyticus</i>	Combination with antibiotics	Roshmi et al. (2015)
Biofilm formation	<i>E. coli</i> , <i>P. aeruginosa</i> , <i>S. aureus</i>	Penetration through biofilm layers and interaction with cellular components	Ramasamy et al. (2017a, b)

(continued)

Table 9.3 (continued)

Type of antibiotic resistance	Targeted bacteria	Mechanisms of antibacterial activity of AuNPs	Ref.
Biofilm formation	<i>E. coli</i> , <i>P. aeruginosa</i> , <i>S. aureus</i> , <i>B. subtilis</i>	ROS generation	Wang et al. (2017a)
Biofilm formation	<i>Proteus</i> species	Interaction between proteins and NPs	Vinoj et al. (2015)
Multidrug resistant	Gram-negative bacteria	Automated microarray-based system for early identification of pathogen and resistance marker detection	Walker et al. (2016)
Multidrug resistant	<i>E. coli</i> , <i>S. aureus</i> , <i>K. pneumoniae</i>	Combination with antibiotics	Vidya et al. (2016)
Multidrug resistant	<i>E. coli</i> , <i>S. aureus</i> , <i>Salmonella typhimurium</i>	Depend on coexisting chemicals that were not removed from AuNPs	Zhang et al. (2015), Dasari et al. (2015)
Multidrug resistant	<i>E. coli</i>	Interaction between lysozyme micro-bubbles and cell wall	Mahalingam et al. (2015)
Multidrug resistant	<i>S. aureus</i> , <i>E. coli</i> , <i>P. aeruginosa</i>	Disruption of bacterial cell wall	Li et al. (2014), Yang et al. (2017)
Multidrug resistant	<i>E. coli</i> , <i>S. aureus</i>	Interaction with biomolecules	Kim et al. (2017)
Multidrug resistant	<i>E. coli</i> , <i>K. pneumoniae</i> , <i>E. cloacae</i>	Photodynamic therapy/ photothermal therapy; Photodynamic therapy/ photothermal therapy	Khan et al. (2017)
Multidrug resistant	<i>S. aureus</i> , <i>E. coli</i> , <i>E. cloacae</i> , <i>P. aeruginosa</i>	Photodynamic therapy/ photothermal therapy	Mocan et al. (2016)
Multidrug resistant	<i>Salmonella typhimurium</i>	Photodynamic therapy/ photothermal therapy	Lin and Hamme II (2015)
Multidrug resistant	<i>S. aureus</i>	Photodynamic therapy/ photothermal therapy	Gil-Tomás et al. (2007)
Multidrug resistant	<i>E. coli</i>	ROS generation	Zhang et al. (2013)
Multidrug resistant	<i>E. coli</i>	Change of membrane potential and inhibition of ATP synthase; inhibition of the subunit of the ribosome for tRNA binding	Cui et al. (2012)
Multidrug resistant	<i>E. coli</i> , <i>K. pneumoniae</i> , <i>S. aureus</i> , <i>B. subtilis</i>	Change of membrane potential and inhibition of ATP synthase; inhibition of the subunit of the ribosome for tRNA binding	Shamaila et al. (2016)

(continued)

Table 9.3 (continued)

Type of antibiotic resistance	Targeted bacteria	Mechanisms of antibacterial activity of AuNPs	Ref.
Multidrug resistant	<i>S. aureus</i>	Photoacoustic detection and photothermal therapy	Galanzha et al. (2012)
Multidrug resistant	<i>E. coli</i> , <i>K. pneumoniae</i>	Not revealed	Bresee et al. (2014)
Multidrug resistant /biofilm formation	<i>P. aeruginosa</i>	Conjugation with AMP	Casciaro et al. (2017)
Multidrug resistant/ biofilm formation	<i>Staphylococci</i> , <i>Enterococci</i> , and other bacterial strain	Conjugation with AMP	Kuo et al. (2016)
Multidrug resistant /biofilm formation	<i>E. coli</i> , <i>S. aureus</i> , <i>K. pneumoniae</i> , <i>P. aeruginosa</i>	Conjugation with AMP	Rai et al. (2017)
Multidrug resistant /biofilm formation	<i>Salmonella typhimurium</i>	Conjugation with AMP	Yeom et al. (2016)

9.4 Mechanism of Antibacterial Activity of Au Nanoparticles

Drug-resistant bacteria acquire genetic modification to exclude antimicrobial drugs and become less sensitive to drugs. To find an effective way to control the threat of bacterial drug resistance, a novel approach to enhance antimicrobial activity is urgently needed. AuNPs are the most studied metal nanoparticles (NPs) for antibacterial applications (Borzenkov et al. 2020). They are biologically inert and pure form of Au does not exert any antibacterial activity (Zhang et al. 2015). However, the surface area of AuNPs is suitable for conjugation with antibiotics and other drugs. A wide range of proteins, drugs, and even nucleotides have also been successfully delivered using AuNPs in the recent past (Perzanowska et al. 2021). Though the exact mechanism underlying the antimicrobial propensity of AuNPs remains unclear, several factors including size, shape, and surface functionalization significantly influence the activity of AuNP.

Major pathways through which AuNPs exert antimicrobial activity include (i) direct contact with bacteria (Shaikh et al. 2019), (ii) physical disruption of membrane (Piktel et al. 2021), (iii) generation of reactive oxygen species (ROS) (Yu et al. 2020), (iv) interaction with cellular proteins and genetic elements (Wang et al. 2015), and (v) trigger host-response immunity (Dykman and Khlebtsov 2017) (Fig. 9.2a). The antimicrobial efficacy of AuNP is largely dependent on their size and shape. The size of the AuNPs plays a critical role in their bactericidal activity, and functionalization with hydrophilic molecule enhances their interaction with bacterial membrane. Hayden et al. reported the size-dependent antimicrobial effect

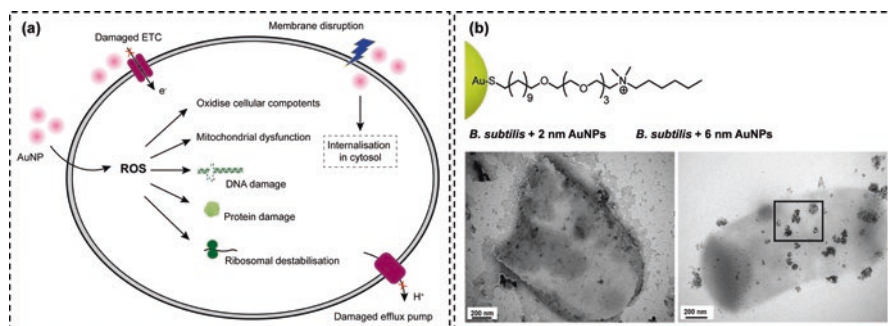


Fig. 9.2 Mechanism of antibacterial activity of AuNPs. (a) AuNPs cause irreversible membrane damage and, hence, particles get internalized in the cytosol. AuNPs then interfere with the cellular components and induce the generation of reactive oxygen species (ROS). ROS brings about different kinds of damage and finally promotes cells to apoptosis. Damaged electron transport chain (ETC) and efflux pump change the electron and proton homeostasis in a cell, respectively. (b) Size-dependent antimicrobial activity of gold (Au) NPs. TEM images confirmed *B. subtilis* membrane rupture by 2 nm AuNPs but not in case of 6 nm NPs. (Reproduced from Hayden et al. (2012) with permission. Copyright © 2012 American Chemical Society)

of cationic AuNPs (Hayden et al. 2012) (Fig. 9.2b). The larger particles (>100 nm) are unable to cross the bacterial membrane; however, smaller particles do and make pores in the membrane (Zheng et al. 2017; Xing et al. 2018).

The large surface area of AuNPs allows the attachment of a wide range of functional elements to enhance the pristine antimicrobial effect. Hence, both AuNPs and their functionalized derivatives have been used to control infections caused by antimicrobial-resistant (AMR) pathogens (Li et al. 2014; Zhao et al. 2013). In addition to increased bactericidal effect, functionalization of the AuNPs' surface also stabilizes the particle and provides prolonged effective and safe drug delivery (Tao 2018). Multivalent Au atom is conjugated with multiple ligands to enhance its antimicrobial activity (Zheng et al. 2017; Ortiz-Benítez et al. 2019). In addition, capping agents used in the synthesis of AuNPs also disrupt cell membrane via electrostatic interactions. AuNPs capped with a mixture of different small molecules can also enhance their antibacterial propensity. For example, AuNPs of 2 nm size capped with p-mercaptobenzoic acid (pMBA-Au) are not effective against bacteria. When pMBAs on the AuNPs' surface are partially replaced with a mixture of 2-mercaptoethylamine and 3-mercaptopropylsulfonate, the resultant AuNPs show 99.9% growth inhibition against *E. coli* at 0.5 mM concentration (Bresee et al. 2011). Li et al. systematically modified the surface of AuNPs to combat multidrug-resistant (MDR) bacteria. Herein, they functionalized 2 nm size AuNPs using hydrophobic molecules having different chain length (Li et al. 2014). The hydrophobic interaction destroys the integrity of bacterial membrane and allows internalization of metal ions, loaded drugs, and protein inhibitors. On the contrary, it also allows the leakage of cytoplasmic content.

The interaction between cationic AuNPs and negatively charged membrane proteins (mostly teichoic acids) results in the aggregation, protrusion and, therefore,

damage the membrane permanently (Hayden et al. 2012; Zhao et al. 2010). The positive charge of AuNPs is responsible for better interaction with negatively charged bacteria which leads to membrane rupture. However, it has been reported that interaction of AuNPs with bacteria changes the membrane permeability, interrupts the electrolyte balance, and deactivates protein function (Wang et al. 2017b). Payne et al. confirmed that the membrane-attached AuNPs penetrate the cell wall of bacteria using small-angle X-ray scattering (Payne et al. 2016). This phenomenon resulted in the disruption of cytosolic environment and leakage of cellular components (Fig. 9.3).

Ortiz-Benítez et al. found that AuNPs reached the cytosolic environment of resistant *S. pneumoniae* and formed spherical cytoplasmic structures known as inclusion bodies (Ortiz-Benítez et al. 2019). They separated the proteins from the inclusion bodies that are potential candidates to facilitate the uptake of NPs in *S. pneumoniae*.

However, conjugation of antibiotics to AuNPs provides enhanced bactericidal effect than pristine AuNPs (Rattanata et al. 2016). Bagga et al. reported that AuNPs-levofloxacin showed greater bactericidal effect against *Staphylococcus aureus*, *Escherichia coli*, and *Pseudomonas aeruginosa* (Payne et al. 2016; Bagga et al. 2017). XX et al. reported a one-pot, fast synthesis of vancomycin-conjugated AuNP which had 16-fold better antibacterial activity against vancomycin-resistant *Enterococci* when compared to free vancomycin (Wang et al. 2018). Other similar

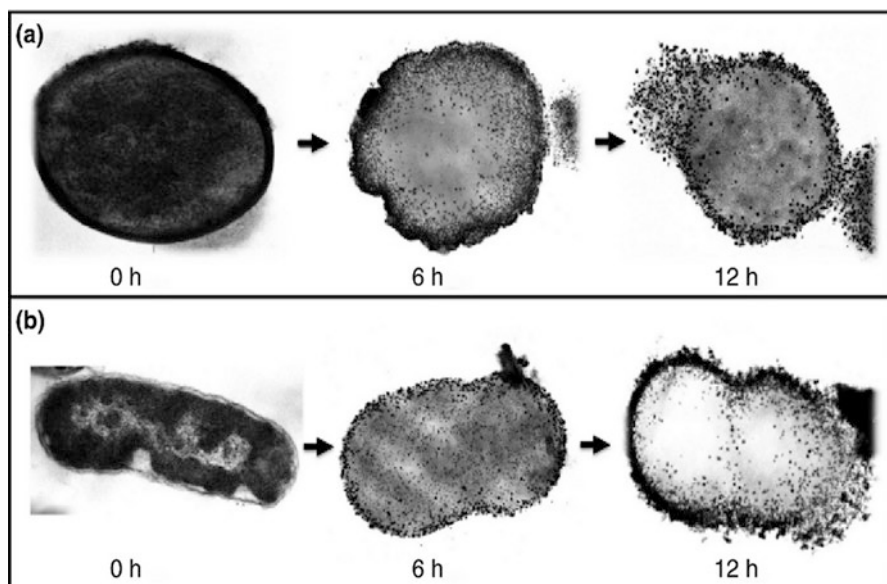


Fig. 9.3 Transmission electron microscopic images of bacteria. Sequential images of gram-positive *Staphylococcus epidermidis* bacteria (a) and gram-negative *Enterobacter aerogenes* bacteria (b) treated with kanamycin-AuNPs after 0, 6, and 12 h of incubation. (Reproduced with permission Payne et al. (2016). Copyright © 2016)

studies also support the codelivery of antibiotics with AuNP to reduce resistance development (Fuller et al. 2020; Justo and Bosso 2015; Sans-Serramitjana et al. 2016; Wang et al. 2020; Fan et al. 2019). Thus, the delivery of antibiotic-conjugated AuNPs not only improve antibacterial efficacy but also require low dose of free antibiotic. Moreover, they also retard bacteria from developing resistance to antibiotics (Chopra 2007). Antibiotic-conjugated AuNPs exert higher antibacterial activity with minimal toxicity (Huh and Kwon 2011). Though synergistic effect of AuNPs-drug conjugate is always discussed as responsible for enhanced antimicrobial activity, the exact mechanism is still unknown. It is hypothesized that this stable conjugation improves internalization of antibiotics to resistant cells (Gu et al. 2003). Only a stable conjugation offers better antibacterial effect. Major drawbacks of antibiotic adsorption on AuNPs include aggregation and poor dispersity of the nanoparticles leading to compound instability. On the other hand, the conjugation of amphiphilic antimicrobial peptides (AMPs) with AuNPs enhances the antibacterial activity of nanoparticles. The advantage of conjugating amphiphilic AMPs is that they facilitate the interaction of AMP-AuNP with bacterial membrane (Wimley and Hristova 2011; Craik et al. 2013; Wadhvani et al. 2017). For example, Lee et al. conjugated hexahistidine-tagged AMPs with aptamer-bound AuNP (Lee et al. 2017). The resultant conjugate was highly effective against infectious pathogens including *Vibrio vulnificus*.

The photothermal property of AuNPs is advantageous for their biomedical applications (Mahmoud et al. 2019). AuNPs produce heat upon illumination with laser, and the thermal energy damages the neighboring bacteria. It is important to make sure that the AuNPs and bacteria are in close proximity so that the photothermal energy generated in the local environment damages the target cell (Mahmoud et al. 2018). Photothermal therapy (PTT) and photodynamic therapy (PDT) are the two main approaches followed by AuNPs to kill bacteria upon laser irradiation. In case of PTT, AuNPs convert the light energy into heat and enhances local temperature to kill bacteria (Jo and Kim 2013; Zhu et al. 2014; Pallavicini et al. 2017). On the other hand, PDT relies on the irradiation of photosensitizers to generate more reactive oxygen species (ROS) that kill bacteria (Venditti 2019). TEM images confirmed the laser-induced bacterial death after treatment with AuNPs. Bermúdez-Jiménez et al. reported the antibacterial effect of chitosan hydrogel-embedded AuNPs against clinical MDR pathogens upon illumination with laser (Bermúdez-Jiménez et al. 2019) and the minimum inhibitory concentration (MIC) was $<4 \mu\text{g/ml}$. The low-power infrared diode laser ruptured the bacterial membrane through enhanced ROS production. The principle of PDT is to generate toxic singlet oxygen upon illumination of photosensitizers with visible light. The highly reactive singlet oxygen damages the neighboring bacterial membrane, interferes with the cellular metabolic pathways, and damages the DNA (Bertoloni et al. 2000; Narband et al. 2009). In recent studies, photosensitizer-embedded AuNPs showed effective antimicrobial activity against both gram-positive and gram-negative bacterial strains (Rossi et al. 2019; Jain et al. 2006; Pallares et al. 2016; Darby et al. 2016; Ni et al. 2008). PDT

is very safe and effective; however, it is highly recommended to deliver therapeutic concentration of the photosensitizers.

Cui et al. investigated the molecular mechanism of bactericidal activity of AuNPs using transcriptomic and proteomic approaches. Two major ways of exerting antibacterial activities include decrease in the cellular ATP level that collapses the membrane potential and the inhibition of tRNA-binding ribosomal protein subunit (Cui et al. 2012). Thus, AuNPs interfere with the activities of ATPase and tRNA. Hence, decoding of mRNA responsible for functional protein enhances ROS-mediated chemotaxis in bacteria and leads to apoptosis (Cui et al. 2012). The most supported mechanism for antibacterial activity of the AuNP is the generation of reactive oxygen species (ROS). These highly reactive chemicals enhance oxidative stress and form vacuoles inside cells (Mohamed et al. 2017).

It is important to highlight that commercially available antibiotics do not follow the multidimensional mode of action like AuNPs to inhibit bacterial growth. Hence, AuNPs can be a good alternative tool to control MDR pathogens. The different mode of antibacterial action of AuNPs is due to the structural differences of gram-positive and gram-negative bacteria (Ranjan Sarker et al. 2019). Hence, AuNPs have a promising future in the field of drug-delivery system (DDS) because delivery of drugs using AuNP is not only effective but also less toxic.

In-depth studies are recommended to unravel the precise mode of action involved in AuNPs-bacteria interaction and their inhibition.

9.5 Biocompatibility of Au Nanoparticles

The field of nanomaterials is expanding rapidly with a wide range of applications (Khan et al. 2019). Besides having several medical applications, AuNPs have toxicities associated with them. Hence, it is very important to know the basic information about the nanomaterials, especially composition, variability of size, shape, surface charge, surface area, surrounding media, and aggregation tendency in biological fluid that influence the biocompatibility of NPs. In this section, properties of Au NPs will be discussed to understand their biocompatibility cell.

A range of techniques have been used to investigate the biocompatibility of AuNPs (Fig. 9.4). Table 9.4 summarizes the principle and benefits of each assay. MTT assay is considered as the “gold standard” to investigate the toxicity of AuNPs. It is a colorimetric assay to determine cellular metabolic activity (Stockert et al. 2018). Herein, enzymatic activity of mitochondrial reductase is monitored under a defined condition. In an oxidation reaction, the enzyme reduces a yellow-colored tetrazolium dye (known as MTT or 3-(4, 5-dimethylthiazol-2-yl)-2, 5-diphenyltetrazolium bromide) and produces insoluble purple-colored formazan. This irreversible reaction reflects the number of live cells at different time points.

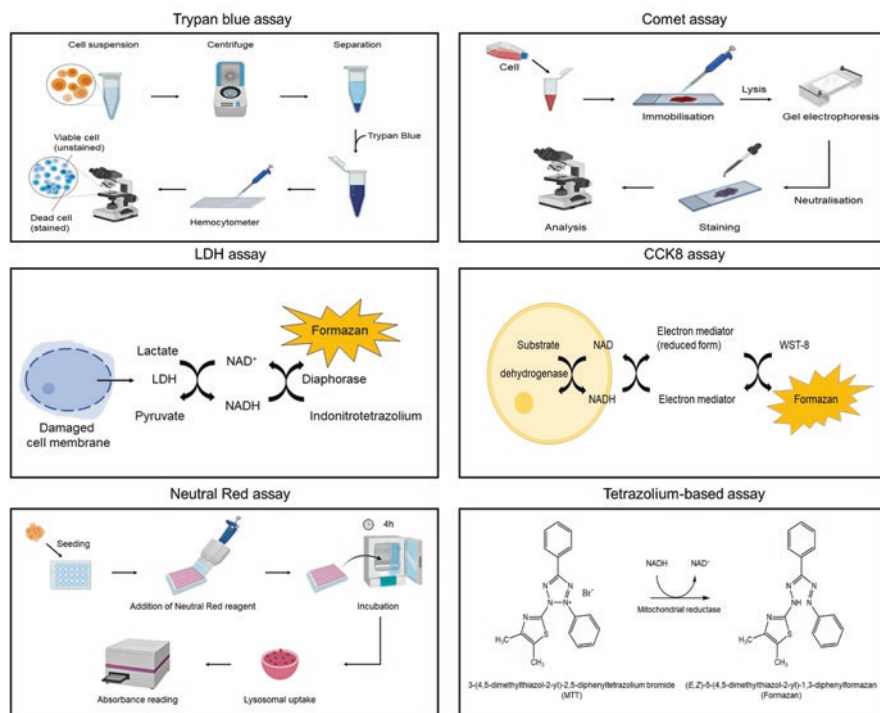


Fig. 9.4 Commonly used assays to determine cell viability

Cell number is quantified by measuring the absorbance of formazan at 570 nm. The degree of formazan production reflects the number of dead cells and is directly proportional to light absorption.

One of the pioneering reports on the biocompatibility assessment of AuNPs was reported by Shukla et al., where the biocompatibility and the uptake of AuNPs by RAW 264.7 macrophage cells were investigated (Shukla et al. 2005). Their findings suggest that AuNPs are highly biocompatible having antioxidation potential at higher doses besides suitable for prolonged treatment. In addition, they found that spherical AuNPs did not induce the secretion of proinflammatory cytokines (e.g., TNF α and interleukin β) by macrophage cells. Chithrani et al. studied the effect of AuNP's shape, size, and toxicity (Chithrani et al. 2006). They concluded that citrate-capped spherical and rod-shaped AuNPs did not cause any significant toxicity to HeLa cells. This study was followed by other research groups and found negligible toxicity for spherical and rod-shaped AuNPs using different cell lines in vitro (Khan et al. 2007; Gu et al. 2009; Villiers et al. 2010). We demonstrated that functionalization of elongated tetrahedral (ETHH) AuNPs with α -lipoic

Table 9.4 Summary of commonly used assays to evaluate the cytotoxicity of AuNPs

Assay	Principle	Remarks	Reference
Trypan blue assay	This diazo dye penetrates the cell membrane of dead cells and stains them selectively	Identifies live (unstained) and dead (blue) cells Provides quantitative cell-to-cell count Fast method Long-time incubation may give false positive result	Strober (2001)
Comet assay	Denatured cleaved DNA fragments migrate out of the cell under electrophoresis and the undamaged DNA remains within the cell membrane	Single-cell gel electrophoresis Economical Sensitive method	Fairbairn et al. (1995)
LDH assay	Colorimetric detection of lactate dehydrogenase (LDH)	Depends on LDH detection Qualitative and quantitative cell count Not preferable for multiple samples	Kumar et al. (2018)
Cell Counting Kit 8 (CCK8)	Cellular dehydrogenases cause reduction of water-soluble tetrazolium salt, WST-8 [2-(2-methoxy-4-nitrophenyl)-3-(4-nitrophenyl)-5-(2,4-disulfophenyl)-2H-tetrazolium, monosodium salt] And produce orange colored formazan	Colorimetric assay No premixing is required Rapid and sensitive Expensive Absorbance interference	Cai et al. (2019)
Neutral Red assay	Incorporation of dye lower in dead cell	Depends on lysosomal function Simple and fast method Quantitative cell count	Repetto et al. (2008)
Tetrazolium-based assays	Conversion of tetrazolium dye to insoluble formazan	Depends on mitochondrial function Colorimetric assay Simple and fast method Qualitative and quantitative cell count Repeatable Economical Not suitable for suspending cells Seeding amount and assay duration must be optimized	Stockert et al. (2018), Vistica et al. (1991)

acid, a natural antioxidant, increased their hemocompatibility as well as biocompatibility to human red blood cells (RBCs) and HeLa cells, respectively (Ranjan Sarker et al. 2019). Recently, we also reported that functionalization of concave cube AuNPs (CCAu) with α -lipoic acid and glutathione, a tripeptide with antioxidant potential, increased their hemocompatibility to human RBCs and biocompatibility to HeLa cells, L929 fibroblasts, and CHO-GFP cells (Pandala et al. 2021). On the contrary, Patra et al. synthesized spherical (33 nm in diameter) AuNPs and investigated their toxicity using three different cell lines (Patra et al. 2007). They found the particles were toxic to human lung carcinoma cells (A549), but compatible with baby hamster kidney cells (BHK21) and human liver carcinoma cells (HepG2).

The hydrodynamic size of AuNPs plays an important role in terms of their cellular uptake and biocompatibility. Earlier studies found that size variability of AuNPs demonstrates negligible toxicity (Khan et al. 2007; Gu et al. 2009; Villiers et al. 2010; Connor et al. 2005). Large AuNPs are generally stable, inactive, non-catalytic, and biocompatible (Khlebtsov and Dykman 2011). Sophisticated tools including inductively coupled plasma mass spectrometry (ICP-MS) are used to quantify AuNPs taken up inside cell (Merrifield et al. 2018). Moreover, electron microscopy confirmed the presence of Au particles in the treated cells (Shukla et al. 2005; García et al. 2013). Chithrani et al. and others studied the cellular uptake of a wide range of AuNPs and quantified the number of nanoparticles inside each cell using inductively coupled plasma atomic emission spectroscopy (Chithrani et al. 2006; Osaki et al. 2004; Huo et al. 2013; Wang et al. 2010; Heuskin et al. 2017). All these studies reported that the maximum uptake was observed in case of 50 nm AuNPs without any cytotoxic effect. Karakoçak et al. used two independent methods (i.e., electric cell-substrate impedance sensing and MTT assay) to investigate the cellular uptake and biocompatibility of spherical, rod-, and cube-shaped AuNPs (Karakoçak et al. 2016). They concluded that sphere-shaped AuNPs have better biocompatibility when compared to Au rods (Fig. 9.5). However, cube-shaped AuNPs neither entered into cells nor had any cytotoxic effect.

Most often rod-shaped AuNPs are synthesized using a cationic surfactant called CTAB. Wang et al. found that free CTAB up to 1 μ M is toxic to mammalian cells (Wang et al. 2008). Therefore, several strategies including chemical exchange or surface functionalization have been chosen to make Au nanorods less toxic. Polyethylene glycol (PEG), a hydrophilic polymer, has been widely used to modify AuNPs' surface. However, PEGylation of AuNPs interferes with the cellular uptake process through reduced endocytosis (Nel et al. 2009; Doak et al. 2009). Chen et al. evaluated intraperitoneally injected eight AuNPs of different size (3–100 nm) and found size dependent toxicity in mice (Chen et al. 2009).

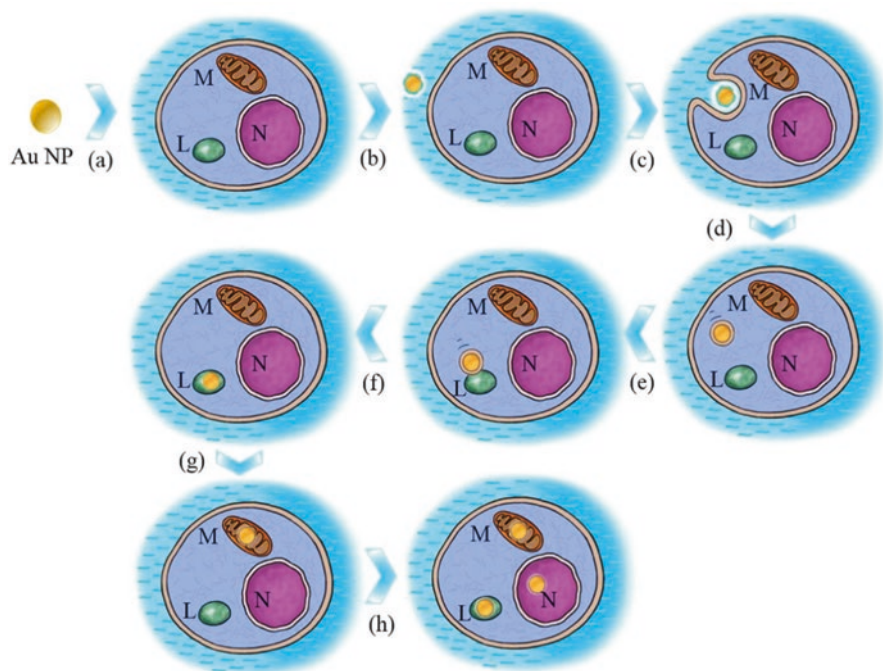


Fig. 9.5 The mechanism of AuNPs-mediated cytotoxicity. (a) Exposure of AuNPs to ARPE-19 cell. (b) Dynamic bipolymer layer (thick and loose blue color coating) creates a superficial surface exposed to the cell membrane. (c,d) Uptake of AuNPs by endocytosis. (e) Fusion of endocytic vesicle with lysosome. (f) Complete internalization of AuNPs by lysosome. (g) AuNPs cross the single membrane of lysosome and penetrate the mitochondrial intermembrane space to initiate apoptosis signal. (h) AuNPs available in the cytoplasm cause cell death by activating subcellular signaling pathways for apoptosis, initiating cell shrinkage, decreasing cytoplasmic shrinkage, and beginning subcellular fragmentation. Here, L lysosome; M mitochondria; and N nucleus. (Reproduced with permission Karakoçak et al. (2016) Copyright © 2016 Elsevier Ltd.)

9.6 Conclusions and Future Perspectives

Multidrug-resistance bacteria are exerting real threat to the existence of mankind because they have become resistant to almost all the commercially available antibiotics. Overuse and misuse of antibiotics are the main causes of the development of bacterial resistance mechanisms against antibiotics. Gold nanoparticles demonstrate antibacterial activity mainly through the oxidation of bacterial membrane resulting in the formation of pores on the membranes. As a result, AuNPs interact with the cellular DNA, proteins, and other macromolecules and cause bacterial death. Since AuNPs demonstrate antibacterial activity by damaging bacterial membrane and other subcellular organelles, they demonstrate antibacterial activity against a wide range of bacteria including pathogenic bacteria and multidrug-resistant bacteria. Furthermore, AuNPs are highly biocompatible in terms of their

compatibility with various cell lines, red blood cells (RBCs), and mouse model (i.e., in vivo). Hence, in clinical trials, AuNPs can be recommended to be used as an alternative nanoweapon to commercially available antibiotics to tackle multidrug-resistant bacteria.

References

- Abdalla SS, Katas H, Azmi F, Busra MFM (2020) Antibacterial and anti-biofilm biosynthesised silver and gold nanoparticles for medical applications: mechanism of action, toxicity and current status. *Curr Drug Deliv* 17(2):88–100
- Adhikari MD, Goswami S, Panda BR, Chattopadhyay A, Ramesh A (2013) Membrane-directed high bactericidal activity of (gold nanoparticle)–polythiophene composite for niche applications against pathogenic bacteria. *Adv Healthc Mater* 2(4):599–606
- Ahmad T, Wani IA, Lone IH, Ganguly A, Manzoor N, Ahmad A, Ahmed J, Al-Shihri AS (2013) Antifungal activity of gold nanoparticles prepared by solvothermal method. *Mater Res Bull* 48(1):12–20
- Allahverdiyev AM, Kon KV, Abamor ES, Bagirova M, Rafailovich M (2011) Coping with antibiotic resistance: combining nanoparticles with antibiotics and other antimicrobial agents. *Expert Rev Anti-Infect Ther* 9(11):1035–1052
- Amin RM, Mohamed MB, Ramadan MA, Verwanger T, Krammer B (2009) Rapid and sensitive microplate assay for screening the effect of silver and gold nanoparticles on bacteria. *Nanomedicine* 4(6):637–643
- Annamalai A, Christina V, Sudha D, Kalpana M, Lakshmi P (2013) Green synthesis, characterization and antimicrobial activity of Au NPs using *Euphorbia hirta* L. leaf extract. *Colloids Surf B* 108:60–65
- Anshup A, Venkataraman JS, Subramaniam C, Kumar RR, Priya S, Kumar TS, Omkumar R, John A, Pradeep T (2005) Growth of gold nanoparticles in human cells. *Langmuir* 21(25):11562–11567
- Arshi N, Ahmed F, Kumar S, Anwar M, Lu J, Koo BH, Lee CG (2011) Microwave assisted synthesis of gold nanoparticles and their antibacterial activity against *Escherichia coli* (E. coli). *Curr Appl Phys* 11(1):S360–S363
- Arunachalam KD, Annamalai SK, Hari S (2013) One-step green synthesis and characterization of leaf extract-mediated biocompatible silver and gold nanoparticles from *Memecylon umbellatum*. *Int J Nanomedicine* 8:1307
- Ashraf S, Pelaz B, del Pino P, Carril M, Escudero A, Parak WJ, Soliman MG, Zhang Q, Carrillo-Carrion C (2016) Gold-based nanomaterials for applications in nanomedicine. In: *Light-responsive nanostructured Systems for Applications in nanomedicine*. Springer International Publishing, Cham, pp 169–202
- Au L, Chen Y, Zhou Y, Camargo PH, Lim B, Li Z-Y, Ginger DS, Xia Y (2008) Synthesis and optical properties of cubic gold nanoframes. *Nano Res* 1(6):441–449
- Averitt R, Sarkar D, Halas N (1997) Plasmon resonance shifts of Au-coated Au 2 S nanoshells: insight into multicomponent nanoparticle growth. *Phys Rev Lett* 78(22):4217
- Azam A, Ahmed F, Arshi N, Chaman M, Naqvi AJIJ (2009) One step synthesis and characterization of gold nanoparticles and their antibacterial activities against *E. coli* (ATCC 25922 strain). *Nanomaterials (Basel)* 1(2):1–4
- Badwaik VD, Vangala LM, Pender DS, Willis CB, Aguilar ZP, Gonzalez MS, Paripelly R, Dakshinamurthy R (2012) Size-dependent antimicrobial properties of sugar-encapsulated gold nanoparticles synthesized by a green method. *Nanoscale Res Lett* 7(1):1–11

- Bagga P, Siddiqui HH, Akhtar J, Mahmood T, Zahera M, Khan MS (2017) Gold nanoparticles conjugated levofloxacin: for improved antibacterial activity over levofloxacin alone. *Curr Drug Deliv* 14(8):1114–1119
- Balagurunathan R, Radhakrishnan M, Rajendran RB, Velmurugan D (2011) Biosynthesis of gold nanoparticles by actinomycete *Streptomyces viridogens* strain HM10
- Balasubramanian K (2014) Antibacterial application of polyvinylalcohol-nanogold composite membranes. *Colloids Surf A* 455:174–178
- Bapat RA, Chaubal TV, Dharmadhikari S, Abdulla AM, Bapat P, Alexander A, Dubey SK, Kesharwani P (2020) Recent advances of gold nanoparticles as biomaterial in dentistry. *Int J Pharm* 586:119596
- Baptista PV, McCusker MP, Carvalho A, Ferreira DA, Mohan NM, Martins M, Fernandes AR (2018) Nano-strategies to fight multidrug resistant bacteria—“a Battle of the titans”. *Front Microbiol* 9:1441
- Basavegowda N, Sobczak-Kupiec A, Malina D, Yathirajan H, Keerthi V, Chandrashekar N, Salman D, Liny P (2013) Plant mediated synthesis of gold nanoparticles using fruit extracts of *Ananas comosus* (L.) (pineapple) and evaluation of biological activities. *Adv Mater Lett* 4:332–337
- Bermúdez-Jiménez C, Romney MG, Roa-Flores SA, Martínez-Castañón G, Bach H (2019) Hydrogel-embedded gold nanorods activated by plasmonic phototherapy with potent antimicrobial activity. *Nanomedicine* 22:102093
- Bertoloni G, Lauro FM, Cortella G, Merchat M (2000) Photosensitizing activity of hematoporphyrin on *Staphylococcus aureus* cells. *Biochim Biophys Acta* 1475(2):169–174
- Bickford LR, Agollah G, Drezek R, Yu T-K (2010) Silica-gold nanoshells as potential intraoperative molecular probes for HER2-overexpression in ex vivo breast tissue using near-infrared reflectance confocal microscopy. *Breast Cancer Res Treat* 120(3):547–555
- Bindhu M, Umadevi M (2014a) Antibacterial activities of green synthesized gold nanoparticles. *Mater Lett* 120:122–125
- Bindhu M, Umadevi M (2014b) Silver and gold nanoparticles for sensor and antibacterial applications. *Spectrochim Acta A* 128:37–45
- Boman H, Wade D, Boman I, Wåhlin B, Merrifield R (1989) Antibacterial and antimalarial properties of peptides that are cecropin-melittin hybrids. *FEBS Lett* 259(1):103–106
- Borah BJ, Yadav A, Dutta DK (2011) Au-nanoparticles: control size and morphology stabilized by tripodal phosphine based ligands and their antimicrobial activity. *J Biomed Nanotechnol* 7(1):152–153
- Borzenkov M, Pallavicini P, Taglietti A, D’Alfonso L, Collini M, Chirico G (2020) Photothermally active nanoparticles as a promising tool for eliminating bacteria and biofilms. *Beilstein J Nanotechnol* 11:1134–1146
- Bresee J, Maier KE, Boncella AE, Melander C, Feldheim DL (2011) Growth inhibition of *Staphylococcus aureus* by mixed monolayer gold nanoparticles. *Small* 7(14):2027–2031
- Bresee J, Bond CM, Worthington RJ, Smith CA, Gifford JC, Simpson CA, Carter CJ, Wang G, Hartman J, Osbaugh NA (2014) Nanoscale structure–activity relationships, mode of action, and biocompatibility of gold nanoparticle antibiotics. *J Am Chem Soc* 136(14):5295–5300
- Brown AN, Smith K, Samuels TA, Lu J, Obare SO, Scott ME (2012) Nanoparticles functionalized with ampicillin destroy multiple-antibiotic-resistant isolates of *Pseudomonas aeruginosa* and *Enterobacter aerogenes* and methicillin-resistant *Staphylococcus aureus*. *Appl Environ Microbiol* 78(8):2768–2774
- Brust M, Walker M, Bethell D, Schiffrin DJ, Whyman R (1994) Chemical communications, synthesis of thiol-derivatised gold nanoparticles in a two-phase liquid–liquid system. *J Chem Soc Chem Commun* 7:801–802
- Busbee BD, Obare SO, Murphy CJ (2003) An improved synthesis of high-aspect-ratio gold nanorods. *Adv Mater* 15(5):414–416
- Cai W, Gao T, Hong H, Sun J (2008) Applications of gold nanoparticles in cancer nanotechnology. *Nanotechnol Sci Appl* 1:17

- Cai L, Qin X, Xu Z, Song Y, Jiang H, Wu Y, Ruan H, Chen J (2019) Comparison of cytotoxicity evaluation of anticancer drugs between real-time cell analysis and CCK-8 method. *ACS Omega* 4(7):12036–12042
- Canizal G, Ascencio J, Gardea-Torresday J, Yacamán MJ (2001) Multiple twinned gold nanorods grown by bio-reduction techniques. *J Nanopart Res* 3(5):475–481
- Caruso F, Spasova M, Salgueiriño-Maceira V, Liz-Marzán L (2001) Multilayer assemblies of silica-encapsulated gold nanoparticles on decomposable colloid templates. *Adv Mater* 13(14):1090–1094
- Casciaro B, Moros M, Rivera-Fernandez S, Bellelli A, Jesús M, Mangoni ML (2017) Gold-nanoparticles coated with the antimicrobial peptide esculentin-1a (1-21) NH₂ as a reliable strategy for antipseudomonal drugs. *Acta Biomater* 47:170–181
- Chang S-S, Shih C-W, Chen C-D, Lai W-C, Wang CC (1999) The shape transition of gold nanorods. *Langmuir* 15(3):701–709
- Chatterjee S, Bandyopadhyay A, Sarkar K (2011) Effect of iron oxide and gold nanoparticles on bacterial growth leading towards biological application. *J Nanobiotechnol* 9(1):1–7
- Chen J, Saeki F, Wiley BJ, Cang H, Cobb MJ, Li Z-Y, Au L, Zhang H, Kimmey MB, Li X (2005) Gold nanocages: bioconjugation and their potential use as optical imaging contrast agents. *Nano Lett* 5(3):473–477
- Chen J, McLellan JM, Siekkinen A, Xiong Y, Li Z-Y, Xia Y (2006) Facile synthesis of gold–silver nanocages with controllable pores on the surface. *J Am Chem Soc* 128(46):14776–14777
- Chen Y-S, Hung Y-C, Liao I, Huang GS (2009) Assessment of the in vivo toxicity of gold nanoparticles. *Nanoscale Res Lett* 4(8):858–864
- Chen W-Y, Lin J-Y, Chen W-J, Luo L, Wei-Guang Diao E, Chen Y-C (2010) Functional gold nanoclusters as antimicrobial agents for antibiotic-resistant bacteria. *Nanomedicine* 5(5):755–764
- Chen Y, Zhang Y, Liang W, Li X (2012) Gold nanocages as contrast agents for two-photon luminescence endomicroscopy imaging. *Nanomedicine* 8(8):1267–1270
- Chithrani BD, Ghazani AA, Chan WC (2006) Determining the size and shape dependence of gold nanoparticle uptake into mammalian cells. *Nano Lett* 6(4):662–668
- Choi CHJ, Alabi CA, Webster P, Davis ME (2010) Mechanism of active targeting in solid tumors with transferrin-containing gold nanoparticles. *Proc Natl Acad Sci* 107(3):1235–1240
- Chopra I (2007) The increasing use of silver-based products as antimicrobial agents: a useful development or a cause for concern? *J Antimicrob Chemother* 59(4):587–590
- Chu Z, Zhang S, Zhang B, Zhang C, Fang C-Y, Rehor I, Cigler P, Chang H-C, Lin G, Liu R (2014) Unambiguous observation of shape effects on cellular fate of nanoparticles. *Sci Rep* 4(1):1–9
- Conde J, Larginho M, Cordeiro A, Raposo LR, Costa PM, Santos S, Diniz MS, Fernandes AR, Baptista PV (2014) Gold-nanobeacons for gene therapy: evaluation of genotoxicity, cell toxicity and proteome profiling analysis. *Nanotoxicology* 8(5):521–532
- Connor EE, Mwamuka J, Gole A, Murphy CJ, Wyatt MD (2005) Gold nanoparticles are taken up by human cells but do not cause acute cytotoxicity. *Small* 1(3):325–327
- Craik DJ, Fairlie DP, Liras S, Price D (2013) The future of peptide-based drugs. *Chem Biol Drug Des* 81(1):136–147
- Cui Y, Zhao Y, Tian Y, Zhang W, Lü X, Jiang X (2012) The molecular mechanism of action of bactericidal gold nanoparticles on *Escherichia coli*. *Biomaterials* 33(7):2327–2333
- Daima HK, Selvakannan P, Shukla R, Bhargava SK, Bansal V (2013) Fine-tuning the antimicrobial profile of biocompatible gold nanoparticles by sequential surface functionalization using polyoxometalates and lysine. *PLoS One* 8(10):e79676
- Daniel M-C, Astruc D (2004) Gold nanoparticles: assembly, supramolecular chemistry, quantum-size-related properties, and applications toward biology, catalysis, and nanotechnology. *Chem Rev* 104(1):293–346
- Darby BL, Auguie B, Meyer M, Pantoja AE, Le Ru EC (2016) Modified optical absorption of molecules on metallic nanoparticles at sub-monolayer coverage. *Nat Photonics* 10(1):40–45
- Das SK, Das AR, Guha AK (2009) Gold nanoparticles: microbial synthesis and application in water hygiene management. *Langmuir* 25(14):8192–8199

- Dasari TS, Zhang Y, Yu H (2015) Antibacterial activity and cytotoxicity of gold (I) and (III) ions and gold nanoparticles. *Biochem Pharmacol* 4(6):199
- Dash SS, Bag BG (2014) Synthesis of gold nanoparticles using renewable Punica granatum juice and study of its catalytic activity. *Appl Nanosci* 4(1):55–59
- Doak SH, Griffiths SM, Manshian B, Singh N, Williams PM, Brown AP, Jenkins GJ (2009) Confounding experimental considerations in nanogenotoxicology. *Mutagenesis* 24(4):285–293
- Dondapati SK, Sau TK, Hrelescu C, Klar TA, Stefani FD, Feldmann J (2010) Label-free biosensing based on single gold nanostars as plasmonic transducers. *ACS Nano* 4(11):6318–6322
- Dreaden EC, Alkilany AM, Huang X, Murphy CJ, El-Sayed MA (2012) The golden age: gold nanoparticles for biomedicine. *Chem Soc Rev* 41(7):2740–2779
- Dykman LA, Khlebtsov NG (2017) Immunological properties of gold nanoparticles. *Chem Sci* 8(3):1719–1735
- El-Batal AI, Hashem A-AM, Abdelbaky NM (2013) Gamma radiation mediated green synthesis of gold nanoparticles using fermented soybean-garlic aqueous extract and their antimicrobial activity. *Springerplus* 2(1):1–10
- Esumi K, Suzuki A, Aihara N, Usui K, Torigoe K (1998) Preparation of gold colloids with UV irradiation using dendrimers as stabilizer. *Langmuir* 14(12):3157–3159
- Fairbairn DW, Olive PL, O'Neill KL (1995) The comet assay: a comprehensive review. *Mutat Res* 339(1):37–59
- Fan Y, Pauer AC, Gonzales AA, Fenniri H (2019) Enhanced antibiotic activity of ampicillin conjugated to gold nanoparticles on PEGylated rosette nanotubes. *Int J Nanomed* 14:7281–7289
- Fang L, Fan H, Guo C, Cui L, Zhang P, Mu H, Xu H, Zhao F, Chen D (2019) Novel mitochondrial targeting multifunctional surface charge-reversal polymeric nanoparticles for cancer treatment. *J Biomed Nanotechnol* 15(11):2151–2163
- Frangioni JV (2003) In vivo near-infrared fluorescence imaging. *Curr Opin Chem Biol* 7(5):626–634
- Freitas de Freitas L, Varca GHC, dos Santos Batista JG, Benévolo Lugão A (2018) An overview of the synthesis of gold nanoparticles using radiation technologies. *Nano* 8(11):939
- Frens G (1973) Controlled nucleation for the regulation of the particle size in monodisperse gold suspensions. *Nat Phys Sci* 241(105):20–22
- Fuller M, Whaley H, Köper I (2020) Antibiotic delivery using gold nanoparticles. *SN Appl Sci* 2(6):1–7
- Galanza EI, Shashkov E, Sarimollaoglu M, Beenken KE, Basnakan AG, Shirtliff ME, Kim J-W, Smeltzer MS, Zharov VP (2012) In vivo magnetic enrichment, photoacoustic diagnosis, and photothermal purging of infected blood using multifunctional gold and magnetic nanoparticles. *PLoS One* 7:e45557
- García CP, Sumbayev V, Gilliland D, Yasinska IM, Gibbs BF, Mehn D, Calzolari L, Rossi F (2013) Microscopic analysis of the interaction of gold nanoparticles with cells of the innate immune system. *Sci Rep* 3(1):1–7
- Geethalakshmi R, Sarada D (2012) Gold and silver nanoparticles from *Trianthema decandra*: synthesis, characterization, and antimicrobial properties. *Int J Nanomedicine* 7:5375
- Geethalakshmi R, Sarada D (2013) Characterization and antimicrobial activity of gold and silver nanoparticles synthesized using saponin isolated from *Trianthema decandra* L. *Ind Crop Prod* 51:107–115
- Giersig M, Mulvaney P (1993) Preparation of ordered colloid monolayers by electrophoretic deposition. *Langmuir* 9(12):3408–3413
- Gil-Tomás J, Tubby S, Parkin IP, Narband N, Dekker L, Nair SP, Wilson M, Street CJ (2007) Lethal photosensitisation of *Staphylococcus aureus* using a toluidine blue O–tiopronin–gold nanoparticle conjugate. *J Mater Chem* 17(35):3739–3746
- Gobin AM, Lee MH, Halas NJ, James WD, Drezek RA, West JL (2007) Near-infrared resonant nanoshells for combined optical imaging and photothermal cancer therapy. *Nano Lett* 7(7):1929–1934

- Gobin AM, Moon JJ, West JL (2008) EphrinA1-targeted nanoshells for photothermal ablation of prostate cancer cells. *Int J Nanomedicine* 3(3):351
- Govindaraju S, Samal M, Yun K (2016) Superior antibacterial activity of GlcN-AuNP-GO by ultraviolet irradiation. *Mater Sci Eng* 69:366–372
- Gu H, Ho P, Tong E, Wang L, Xu B (2003) Presenting vancomycin on nanoparticles to enhance antimicrobial activities. *Nano Lett* 3(9):1261–1263
- Gu YJ, Cheng J, Lin CC, Lam YW, Cheng SH, Wong WT (2009) Nuclear penetration of surface functionalized gold nanoparticles. *Toxicol Appl Pharmacol* 237(2):196–204
- Hainfeldt JF, Dilmanian FA, Slatkin DN, Smilowitz HM (2008) Radiotherapy enhancement with gold nanoparticles. *J Pharm Pharmacol* 60(8):977–985
- Hao F, Nehl CL, Hafner JH, Nordlander P (2007) Plasmon resonances of a gold nanostar. *Nano Lett* 7(3):729–732
- Hayden SC, Zhao G, Saha K, Phillips RL, Li X, Miranda OR, Rotello VM, El-Sayed MA, Schmidt-Krey I, Bunz UH (2012) Aggregation and interaction of cationic nanoparticles on bacterial surfaces. *J Am Chem Soc* 134(16):6920–6923
- Hernández-Sierra JF, Ruiz F, Pena DCC, Martínez-Gutiérrez F, Martínez AE, Guillén ADJP, Tapiá-Pérez H, Castañón GM (2008) Biology; medicine, the antimicrobial sensitivity of *Streptococcus mutans* to nanoparticles of silver, zinc oxide, and gold. *Nanomedicine* 4(3):237–240
- Heuskin AC, Gallez B, Feron O, Martinive P, Michiels C, Lucas S (2017) Metallic nanoparticles irradiated by low-energy protons for radiation therapy: are there significant physical effects to enhance the dose delivery? *Med Phys* 44(8):4299–4312
- Hirsch LR, Stafford RJ, Bankson J, Sershen SR, Rivera B, Price R, Hazle JD, Halas NJ, West JL (2003) Nanoshell-mediated near-infrared thermal therapy of tumors under magnetic resonance guidance. *Proc Natl Acad Sci* 100(23):13549–13554
- Hossain M, Polash SA, Takikawa M, Shubhra RD, Saha T, Islam Z, Hossain M, Hasan M, Takeoka S, Sarker SR (2019) Investigation of the antibacterial activity and in vivo cytotoxicity of biogenic silver nanoparticles as potent therapeutics. *Front Bioeng Biotechnol* 7:239
- Hrelescu C, Sau TK, Rogach AL, Jäckel F, Feldmann J (2009) Single gold nanostars enhance Raman scattering. *Appl Phys Lett* 94(15):153113
- Hu D, Li H, Wang B, Ye Z, Lei W, Jia F, Jin Q, Ren K-F, Ji J (2017) Surface-adaptive gold nanoparticles with effective adherence and enhanced photothermal ablation of methicillin-resistant *Staphylococcus aureus* biofilm. *ACS Nano* 11(9):9330–9339
- Huang P, Bao L, Zhang C, Lin J, Luo T, Yang D, He M, Li Z, Gao G, Gao B (2011). *Biomaterials* 32(36):9796–9809
- Huh AJ, Kwon YJ (2011) “Nanoantibiotics”: a new paradigm for treating infectious diseases using nanomaterials in the antibiotics resistant era. *J Control Release* 156(2):128–145
- Huo S, Ma H, Huang K, Liu J, Wei T, Jin S, Zhang J, He S, Liang XJ (2013) Superior penetration and retention behavior of 50 nm gold nanoparticles in tumors. *Cancer Res* 73(1):319–330
- Jain PK, Lee KS, El-Sayed IH, El-Sayed MA (2006) Calculated absorption and scattering properties of gold nanoparticles of different size, shape, and composition: applications in biological imaging and biomedicine. *J Phys Chem B* 110(14):7238–7248
- Jana NR, Gearheart L, Murphy CJ (2001a) Wet chemical synthesis of high aspect ratio cylindrical gold nanorods. *J Phys Chem B* 105(19):4065–4067
- Jana NR, Gearheart L, Murphy CJ (2001b) Seed-mediated growth approach for shape-controlled synthesis of spheroidal and rod-like gold nanoparticles using a surfactant template. *Adv Mater* 13(18):1389–1393
- Jana NR, Gearheart L, Obare SO, Murphy CJ (2002) Anisotropic chemical reactivity of gold spheroids and nanorods. *Langmuir* 18(3):922–927
- Jo W, Kim MJ (2013) Influence of the photothermal effect of a gold nanorod cluster on biofilm disinfection. *Nanotechnology* 24(19):195104
- Justo JA, Bosso JA (2015) Adverse reactions associated with systemic polymyxin therapy. *Pharmacotherapy* 35(1):28–33

- Karakoçak BB, Raliya R, Davis JT, Chavalmane S, Wang WN, Ravi N, Biswas P (2016) Biocompatibility of gold nanoparticles in retinal pigment epithelial cell line. *Toxicol In Vitro* 37:61–69
- Khan JA, Pillai B, Das TK, Singh Y, Maiti S (2007) Molecular effects of uptake of gold nanoparticles in HeLa cells. *Chembiochem* 8(11):1237–1240
- Khan S, Khan SN, Meena R, Dar AM, Pal R, Khan AU (2017) Photoinactivation of multidrug resistant bacteria by monomeric methylene blue conjugated gold nanoparticles. *J Photochem Photobiol B* 174:150–161
- Khan I, Saeed K, Khan I (2019) Nanoparticles: properties, applications and toxicities. *Arab J Chem* 12(7):908–931
- Khlebtsov N, Dykman L (2011) Biodistribution and toxicity of engineered gold nanoparticles: a review of in vitro and in vivo studies. *Chem Soc Rev* 40(3):1647–1671
- Kim Y-P, Oh E, Hong M-Y, Lee D, Han M-K, Shon HK, Moon DW, Kim H-S, Lee TG (2006) Gold nanoparticle-enhanced secondary ion mass spectrometry imaging of peptides on self-assembled monolayers. *Anal Chem* 78(6):1913–1920
- Kim D-Y, Kim M, Shinde S, Sung J-S, Ghodake G (2017) Cytotoxicity and antibacterial assessment of gallic acid capped gold nanoparticles. *Colloids Surf B* 149:162–167
- Kodiha M, Hutter E, Boridy S, Juhas M, Maysinger D, Stochaj U (2014) Gold nanoparticles induce nuclear damage in breast cancer cells, which is further amplified by hyperthermia. *Cell Mol Life Sci* 71(21):4259–4273
- Kumar P, Nagarajan A, Uchil PD (2018) Analysis of cell viability by the lactate dehydrogenase assay. *Cold Spring Harb Protoc* 2018(6):pdb-prot095497
- Kundu S (2017) Gold nanoparticles: their application as antimicrobial agents and vehicles of gene delivery. *Adv Biotechnol Microbiol* 4:556–558
- Kuo W-S, Chang C-N, Chang Y-T, Yeh C-S (2009) Antimicrobial gold nanorods with dual-modality photodynamic inactivation and hyperthermia. *Chem Commun* 32:4853–4855
- Kuo Y-L, Wang S-G, Wu C-Y, Lee K-C, Jao C-J, Chou S-H, Chen Y-C (2016) Functional gold nanoparticle-based antibacterial agents for nosocomial and antibiotic-resistant bacteria. *Nanomedicine* 11(19):2497–2510
- Kwon MJ, Lee J, Wark AW, Lee HJ (2012) Nanoparticle-enhanced surface plasmon resonance detection of proteins at attomolar concentrations: comparing different nanoparticle shapes and sizes. *Anal Chem* 84(3):1702–1707
- Lai H-Z, Chen W-Y, Wu C-Y, Chen Y-C (2015) Potent antibacterial nanoparticles for pathogenic bacteria. *ACS Appl Mater Interfaces* 7(3):2046–2054
- Lee B, Park J, Ryu M, Kim S, Joo M, Yeom JH, Kim S, Park Y, Lee K, Bae J (2017) Antimicrobial peptide-loaded gold nanoparticle-DNA aptamer conjugates as highly effective antibacterial therapeutics against *Vibrio vulnificus*. *Sci Rep* 7(1):13572
- Leff DV, Brandt L, Heath JR (1996) Synthesis and characterization of hydrophobic, organically-soluble gold nanocrystals functionalized with primary amines. *Langmuir* 12(20):4723–4730
- Li X, Robinson SM, Gupta A, Saha K, Jiang Z, Moyano DF, Sahar A, Riley MA, Rotello VM (2014) Functional gold nanoparticles as potent antimicrobial agents against multi-drug-resistant bacteria. *ACS Nano* 8(10):10682–10686
- Lima E, Guerra R, Lara V, Guzmán AJCCJ (2013) Gold nanoparticles as efficient antimicrobial agents for *Escherichia coli* and *salmonella typhi*. *Chem Cent J* 7(1):1–7
- Lin Y, Hamme AT II (2015) Gold nanoparticle labeling based ICP-MS detection/measurement of bacteria, and their quantitative photothermal destruction. *J Mater Chem B* 3(17):3573–3582
- Liny P, Divya T, Malakar B, Nagaraj B, Krishnamurthy N, Dinesh R (2012) Preparation of gold nanoparticles from *Helianthus annuus* (sun flower) flowers and evaluation of their antimicrobial activities. *Int J Pharm Bio Sci* 3(1):439–446
- Lokina S, Suresh R, Giribabu K, Stephen A, Sundaram RL, Narayanan V (2014) Spectroscopic investigations, antimicrobial, and cytotoxic activity of green synthesized gold nanoparticles. *Spectrochim Acta A* 129:484–490

- Loo C, Hirsch L, Lee M-H, Chang E, West J, Halas N, Drezek R (2005) Gold nanoshell bioconjugates for molecular imaging in living cells. *Opt Lett* 30(9):1012–1014
- Lowery AR, Gobin AM, Day ES, Halas NJ, West JL (2006) Immunonanoshells for targeted photothermal ablation of tumor cells. *Int J Nanomedicine* 1(2):149
- Lu X, Chen J, Skrabalak S, Xia Y (2007) Nanosystems, galvanic replacement reaction: a simple and powerful route to hollow and porous metal nanostructures. *Proc Inst Mech Eng, Part N* 221(1):1–16
- Mahalingam S, Xu Z, Edirisinghe M (2015) Antibacterial activity and biosensing of PVA-lysozyme microbubbles formed by pressurized gyration. *Langmuir* 31(36):9771–9780
- Mahitha B, Raju BDP, Madhavi T, Lakshmi CNM, Sushma NJ (2013) Evaluation of antibacterial efficacy of phyto fabricated gold nanoparticles using bacopa monniera plant extract. *Ind J Adv Chem Sci* 1(2):94–98
- Mahmoud MA, El-Sayed MA (2010) Gold nanoframes: very high surface plasmon fields and excellent near-infrared sensors. *J Am Chem Soc* 132(36):12704–12710
- Mahmoud M, Snyder B, El-Sayed M (2010) Surface plasmon fields and coupling in the hollow gold nanoparticles and surface-enhanced Raman spectroscopy. Theory and experiment. *J Phys Chem C* 114(16):7436–7443
- Mahmoud NN, Alkilany AM, Khalil EA, Al-Bakri AG (2018) Nano-photothermal ablation effect of hydrophilic and hydrophobic functionalized gold nanorods on *Staphylococcus aureus* and *Propionibacterium acnes*. *Sci Rep* 8(1):6881
- Mahmoud NN, Alhusban AA, Ali JI, Al-Bakri AG, Hamed R, Khalil EA (2019) Preferential accumulation of phospholipid-PEG and cholesterol-PEG decorated gold nanorods into human skin layers and their photothermal-based antibacterial activity. *Sci Rep* 9(1):5796
- Marangoni VS, Paino IM, Zucolotto V (2013) Synthesis and characterization of jacalin-gold nanoparticles conjugates as specific markers for cancer cells. *Colloids Surf B* 112:380–386
- Martin CRS (1994) Nanomaterials: a membrane-based synthetic approach. *Science* 266(5193):1961–1966
- Mendes R, Pedrosa P, Lima JC, Fernandes AR, Baptista PV (2017) Photothermal enhancement of chemotherapy in breast cancer by visible irradiation of gold nanoparticles. *Sci Rep* 7(1):1–9
- Merchant B (1998) Gold, the noble metal and the paradoxes of its toxicology. *Biologicals* 26(1):49–59
- Merrifield RC, Stephan C, Lead JR (2018) Quantification of Au nanoparticle biouptake and distribution to freshwater algae using single cell - ICP-MS. *Environ Sci Technol* 52(4):2271–2277
- Mieszawska AJ, Zamborini FP (2005) Gold nanorods grown directly on surfaces from microscale patterns of gold seeds. *Chem Mater* 17(13):3415–3420
- Millenbaugh NJ, Baskin JB, DeSilva MN, Elliott WR, Glickman RD (2015) Photothermal killing of *Staphylococcus aureus* using antibody-targeted gold nanoparticles. *Int J Nanomed* 10:1953
- Mishra A, Tripathy SK, Yun S-I (2011) Bio-synthesis of gold and silver nanoparticles from *Candida guilliermondii* and their antimicrobial effect against pathogenic bacteria. *J Nanosci Nanotechnol* 11(1):243–248
- Mishra A, Kumari M, Pandey S, Chaudhry V, Gupta K, Nautiyal C (2014) Biocatalytic and antimicrobial activities of gold nanoparticles synthesized by *Trichoderma* sp. *Bioresour Technol* 166:235–242
- Mitra P, Chakraborty PK, Saha P, Ray P, Basu S (2014) Antibacterial efficacy of acridine derivatives conjugated with gold nanoparticles. *Int J Pharm* 473(1–2):636–643
- Mocan L, Matea C, Tabaran FA, Mosteanu O, Pop T, Puia C, Agoston-Coldea L, Gonciar D, Kalman E, Zaharie G (2016) Selective in vitro photothermal nano-therapy of MRSA infections mediated by IgG conjugated gold nanoparticles. *Sci Rep* 6(1):1–9
- Mocan L, Tabaran FA, Mocan T, Pop T, Mosteanu O, Agoston-Coldea L, Matea CT, Gonciar D, Zdrehus C, Iancu C (2017) Laser thermal ablation of multidrug-resistant bacteria using functionalized gold nanoparticles. *Int J Nanomedicine* 12:2255

- Mohamed MM, Fouad SA, Elshoky HA, Mohammed GM, Salaheldin TA (2017) Antibacterial effect of gold nanoparticles against *Corynebacterium pseudotuberculosis*. *Int J Vet Sci Med* 5(1):23–29
- Mollick MMR, Bhowmick B, Mondal D, Maity D, Rana D, Dash SK, Chattopadhyay S, Roy S, Sarkar J, Acharya K (2014) Anticancer (in vitro) and antimicrobial effect of gold nanoparticles synthesized using *Abelmoschus esculentus* (L.) pulp extract via a green route. *RSC Adv* 4(71):37838–37848
- Moreno-Álvarez S, Martínez-Castañón G, Niño-Martínez N, Reyes-Macías J, Patiño-Marín N, Loyola-Rodríguez J, Ruiz F (2010) Preparation and bactericide activity of gallic acid stabilized gold nanoparticles. *J Nanopart Res* 12(8):2741–2746
- MubarakAli D, Thajuddin N, Jeganathan K, Gunasekaran M (2011) Plant extract mediated synthesis of silver and gold nanoparticles and its antibacterial activity against clinically isolated pathogens. *Colloids Surf B* 85(2):360–365
- Mukha I, Eremenko A, Korchak G, Michienkova A (2010) Antibacterial action and physicochemical properties of stabilized silver and gold nanostructures on the surface of disperse silica. *J Water Resour Prot* 2:131–136
- Mukherjee P, Ahmad A, Mandal D, Senapati S, Sainkar SR, Khan MI, Ramani R, Parischa R, Ajayakumar P, Alam M, Sastry M (2001) Bioreduction of AuCl₄⁻ ions by the fungus, *Verticillium* sp. and surface trapping of the gold nanoparticles formed. *Angew Chem Int Ed* 40(19):3585–3588
- Nagajyothi P, Sreekanth T, Prasad T, Lee KD (2012) Harvesting Au nanoparticles from *Carthamus tinctorius* flower extract and evaluation of their antimicrobial activity. *Adv Sci Lett* 5(1):124–130
- Nagaraj B, Divya T, Krishnamurthy N, Dinesh R, Negrila C, Predoi D (2012) Phytosynthesis of gold nanoparticles using *caesalpinia pulcherrima* (peacock flower) flower extract and evaluation of their antimicrobial activities. *J Optoelectron Adv Mater* 7(3)
- Naik AJ, Ismail S, Kay C, Wilson M, Parkin IP (2011) Antimicrobial activity of polyurethane embedded with methylene blue, toluidene blue and gold nanoparticles against *Staphylococcus aureus*; illuminated with white light. *Mater Chem Phys* 129(1–2):446–450
- Narband N, Uppal M, Dunnill CW, Hyett G, Wilson M, Parkin IP (2009) The interaction between gold nanoparticles and cationic and anionic dyes: enhanced UV-visible absorption. *Phys Chem Chem Phys* 11(44):10513–10518
- Naveena BE, Prakash S (2013) Biological synthesis of gold nanoparticles using marine algae *Gracilaria corticata* and its application as a potent antimicrobial and antioxidant agent. *Asian J Pharm Clin* 6(2):179–182
- Nazari ZE, Banoee M, Sepahi AA, Rafii F, Shahverdi AR (2012) The combination effects of trivalent gold ions and gold nanoparticles with different antibiotics against resistant *Pseudomonas aeruginosa*. *Gold Bull* 45(2):53–59
- Nel AE, Mädler L, Velegol D, Xia T, Hoek EM, Somasundaran P, Klaessig F, Castranova V, Thompson M (2009) Understanding biophysicochemical interactions at the nano-bio interface. *Nat Mater* 8(7):543–557
- Ni W, Yang Z, Chen H, Li L, Wang J (2008) Coupling between molecular and plasmonic resonances in freestanding dye-gold nanorod hybrid nanostructures. *J Am Chem Soc* 130(21):6692–6693
- Nichols JW, Bae YH (2014) EPR: evidence and fallacy. *J Control Release* 190:451–464
- Niloy MS, Hossain MM, Takikawa M, Shakil MS, Polash SA, Mahmud KM, Uddin MF, Alam M, Shubhra RD, Shawan MMAK, Saha T (2020) Synthesis of biogenic silver nanoparticles using *caesalpinia digyna* and investigation of their antimicrobial activity and in vivo biocompatibility. *ACS Appl Biol Mater* 3:7722–7733
- Ocoy I, Yusufbeyoglu S, Yilmaz V, McLamore ES, Ildiz N, Ülgen A (2017) DNA aptamer functionalized gold nanostructures for molecular recognition and photothermal inactivation of methicillin-resistant *Staphylococcus aureus*. *Colloids Surf B* 159:16–22
- Oldenburg S, Averitt R, Westcott S, Halas NJ (1998) Nanoengineering of optical resonances. *Chem Phys Lett* 288(2–4):243–247

- Oldenburg SJ, Westcott SL, Averitt RD, Halas NJ (1999a) Surface enhanced Raman scattering in the near infrared using metal nanoshell substrates. *J Chem Phys* 111(10):4729–4735
- Oldenburg SJ, Jackson JB, Westcott SL, Halas NJ (1999b) Infrared extinction properties of gold nanoshells. *Appl Phys Lett* 75(19):2897–2899
- Ortiz-Benítez EA, Velázquez-Guadarrama N, Durán Figueroa NV, Quezada H, Olivares-Trejo JJ (2019) Antibacterial mechanism of gold nanoparticles on *Streptococcus pneumoniae*. *Metallomics* 11(7):1265–1276
- Osaki F, Kanamori T, Sando S, Sera T, Aoyama Y (2004) A quantum dot conjugated sugar ball and its cellular uptake. On the size effects of endocytosis in the subviral region. *J Am Chem Soc* 126(21):6520–6521
- Pal S, Mitra K, Azmi S, Ghosh JK, Chakraborty TK (2011) Towards the synthesis of sugar amino acid containing antimicrobial noncytotoxic CAP conjugates with gold nanoparticles and a mechanistic study of cell disruption. *Org Biomol Chem* 9(13):4806–4810
- Pallares RM, Su X, Lim SH, Thanh NT (2016) Fine-tuning of gold nanorod dimensions and plasmonic properties using the Hofmeister effects. *J Mater Chem C* 4(1):53–61
- Pallavicini P, Dona A, Taglietti A, Minzioni P, Patrini M, Dacarro G, Chirico G, Sironi L, Bloise N, Visai L (2014) Self-assembled monolayers of gold nanostars: a convenient tool for near-IR photothermal biofilm eradication. *Chem Commun* 50(16):1969–1971
- Pallavicini P, Bassi B, Chirico G, Collini M, Dacarro G, Fratini E, Grisoli P, Patrini M, Sironi L, Taglietti A, Moritz M, Sorzabal-Bellido I, Susarrey-Arce A, Latter E, Beckett AJ, Prior IA, Raval R, Diaz Fernandez YA (2017) Modular approach for bimodal antibacterial surfaces combining photo-switchable activity and sustained biocidal release. *Sci Rep* 7(1):5259
- Pandala N, LaScola MA, Tang Y, Bieberich M, Korley LT, Lavik E (2021) Screen printing tissue models using chemically cross-linked hydrogel systems: a simple approach to efficiently make highly tunable matrices. *ACS Biomater Sci Eng* 7(11):5007–5013
- Park J, Estrada A, Sharp K, Sang K, Schwartz JA, Smith DK, Coleman C, Payne JD, Korgel BA, Dunn AK (2008) Two-photon-induced photoluminescence imaging of tumors using near-infrared excited gold nanoshells. *Opt Express* 16(3):1590–1599
- Patra HK, Banerjee S, Chaudhuri U, Lahiri P, Dasgupta AK (2007) Cell selective response to gold nanoparticles. *Nanomedicine* 3(2):111–119
- Payne JN, Waghvani HK, Connor MG, Hamilton W, Tockstein S, Moolani H, Chavda F, Badwaik V, Lawrenz MB, Dakshinamurthy R (2016) Novel synthesis of kanamycin conjugated gold nanoparticles with potent antibacterial activity. *Front Microbiol* 7:607
- Perzanowska O, Majewski M, Strenkowska M, Głowala P, Czarnocki-Cieciura M, Mazur M, Kowalska J, Jemielity J (2021) Nucleotide-decorated AuNPs as probes for nucleotide-binding proteins. *Sci Rep* 11(1):15741
- Piktel E, Suprewicz Ł, Depciuch J, Chmielewska S, Skłodowska K, Daniluk T, Król G, Kołat-Brodecka P, Bijak P, Pajor-Świerzy A, Fiedoruk K, Parlinska-Wojtan M, Bucki R (2021) Varied-shaped gold nanoparticles with nanogram killing efficiency as potential antimicrobial surface coatings for the medical devices. *Sci Rep* 11(1):12546
- Podsiadlo P, Sinani VA, Bahng JH, Kam NWS, Lee J, Kotov NA (2008) Gold nanoparticles enhance the anti-leukemia action of a 6-mercaptopurine chemotherapeutic agent. *Langmuir* 24(2):568–574
- Polash SA, Hossain M, Saha T, Sarker SR (2021) Biogenic silver nanoparticles: a potent therapeutic agent. In: *Emerging trends in nanomedicine*. Springer, Berlin, pp 81–127
- Radloff C, Vaia RA, Brunton J, Bouwer GT, Ward VK (2005) Metal nanoshell assembly on a virus bioscaffold. *Nano Lett* 5(6):1187–1191
- Rai A, Pinto S, Velho TR, Ferreira AF, Moita C, Trivedi U, Evangelista M, Comune M, Rumbaugh KP, Simões PN (2016) One-step synthesis of high-density peptide-conjugated gold nanoparticles with antimicrobial efficacy in a systemic infection model. *Biomaterials* 85:99–110
- Rai M, Ingle AP, Pandit R, Paralikar P, Gupta I, Chaud MV, Dos Santos CA (2017) Broadening the spectrum of small-molecule antibacterials by metallic nanoparticles to overcome microbial resistance. *Int J Pharm* 532(1):139–148

- Rajchakit U, Sarojini V (2017) Recent developments in antimicrobial-peptide-conjugated gold nanoparticles. *Bioconjug Chem* 28(11):2673–2686
- Ramamurthy C, Padma M, Mareeswaran R, Suyavaran A, Kumar MS, Premkumar K, Thirunavukkarasu C (2013) The extra cellular synthesis of gold and silver nanoparticles and their free radical scavenging and antibacterial properties. *Colloids Surf B* 102:808–815
- Ramasamy M, Lee J-H, Lee J (2017a) Direct one-pot synthesis of cinnamaldehyde immobilized on gold nanoparticles and their antibiofilm properties. *Colloids Surf B* 160:639–648
- Ramasamy M, Lee J-H, Lee J (2017b) Development of gold nanoparticles coated with silica containing the antibiofilm drug cinnamaldehyde and their effects on pathogenic bacteria. *Int J Nanomed* 12:2813
- Ranjan Sarker S, Polash SA, Boath J, Kandjani AE, Poddar A, Dekiwadia C, Shukla R, Sabri Y, Bhargava SK (2019) Functionalization of elongated tetrahedral Au nanoparticles and their antimicrobial activity assay. *ACS Appl Mater Interfaces* 11(14):13450–13459
- Rattanata N, Klaynongsruang S, Leelayuwat C, Limpaboon T, Lulitanond A, Boonsiri P, Chio-Srichan S, Soontaranon S, Rugmai S, Daduang J (2016) Gallic acid conjugated with gold nanoparticles: antibacterial activity and mechanism of action on foodborne pathogens. *Int J Nanomedicine* 11:3347–3356
- Reetz MT, Helbig W (1994) Size-selective synthesis of nanostructured transition metal clusters. *J Am Chem Soc* 116(16):7401–7402
- Repetto G, del Peso A, Zurita JL (2008) Neutral red uptake assay for the estimation of cell viability/cytotoxicity. *Nat Protoc* 3(7):1125–1131
- Rodríguez-Lorenzo L, Alvarez-Puebla RA, Pastoriza-Santos I, Mazzucco S, Stéphan O, Kociak M, Liz-Marzán LM, García de Abajo FJ (2009) Zeptomol detection through controlled ultrasensitive surface-enhanced Raman scattering. *J Am Chem Soc* 131(13):4616–4618
- Roshmi T, Soumya K, Jyothis M, Radhakrishnan E (2015) Effect of biofabricated gold nanoparticle-based antibiotic conjugates on minimum inhibitory concentration of bacterial isolates of clinical origin. *Gold Bull* 48(1):63–71
- Rossi F, Thanh NTK, Su XD (2019) Gold nanorods embedded in polymeric film for killing bacteria by generating reactive oxygen species with light. *ACS Appl Biol Mater* 2(7):3059–3067
- Rossolini GM, Arena F, Pecile P, Pollini S (2014) Update on the antibiotic resistance crisis. *Curr Opin Pharmacol* 18:56–60
- Sans-Serramitjana E, Fusté E, Martínez-Garriga B, Merlos A, Pastor M, Pedraz JL, Esquisabel A, Bachiller D, Vinuesa T, Viñas M (2016) Killing effect of nanoencapsulated colistin sulfate on *Pseudomonas aeruginosa* from cystic fibrosis patients. *J Cyst Fibros* 15(5):611–618
- Selvaraj V, Grace AN, Alagar M, Hamerton I (2010) Antimicrobial and anticancer efficacy of anti-neoplastic agent capped gold nanoparticles. *J Biomed Nanotechnol* 6(2):129–137
- Shaikh S, Rizvi SMD, Shakil S, Hussain T, Alshammari TM, Ahmad W, Tabrez S, Al-Qahtani MH, Abuzenadah AM (2017) Synthesis and characterization of cefotaxime conjugated gold nanoparticles and their use to target drug-resistant CTX-M-producing bacterial pathogens. *J Cell Biochem* 118(9):2802–2808
- Shaikh S, Nazam N, Rizvi SMD, Ahmad K, Baig MH, Lee EJ, Choi I (2019) Mechanistic insights into the antimicrobial actions of metallic nanoparticles and their implications for multidrug resistance. *Int J Mol Sci* 20(10):2468
- Shaker MA, Shaaban MI (2017) Formulation of carbapenems loaded gold nanoparticles to combat multi-antibiotic bacterial resistance: in vitro antibacterial study. *Int J Pharm* 525(1):71–84
- Shamaila S, Zafar N, Riaz S, Sharif R, Nazir J, Naseem S (2016) Gold nanoparticles: an efficient antimicrobial agent against enteric bacterial human pathogen. *J Nano* 6(4):71
- Shankar SS, Rai A, Ahmad A, Sastry MJ (2004) Rapid synthesis of Au, Ag, and bimetallic Au core–Ag shell nanoparticles using Neem (*Azadirachta indica*) leaf broth. *J Colloid Interface Sci* 275(2):496–502
- Shankar S, Jaiswal L, Aparna R, Prasad R (2014) Synthesis, characterization, in vitro biocompatibility, and antimicrobial activity of gold, silver and gold silver alloy nanoparticles prepared from *Lansium domesticum* fruit peel extract. *Mater Lett* 137:75–78

- Shukla R, Bansal V, Chaudhary M, Basu A, Bhonde RR, Sastry M (2005) Biocompatibility of gold nanoparticles and their endocytotic fate inside the cellular compartment: a microscopic overview. *Langmuir* 21(23):10644–10654
- Skrabalak SE, Au L, Li X, Xia Y (2007) Facile synthesis of Ag nanocubes and Au nanocages. *Nat Protoc* 2(9):2182–2190
- Skrabalak SE, Chen J, Sun Y, Lu X, Au L, Cobley CM, Xia Y (2008) Gold nanocages: synthesis, properties, and applications. *Acc Chem Res* 41(12):1587–1595
- Smitha S, Gopchandran KG (2013) Surface enhanced Raman scattering, antibacterial and antifungal active triangular gold nanoparticles. *Spectrochim Acta A* 102:114–119
- Sreekanth T, Nagajyothi P, Lee KD (2012) Biosynthesis of gold nanoparticles and their antimicrobial activity and cytotoxicity. *Adv Sci Lett* 6(1):63–69
- Sreekanth T, Nagajyothi P, Supraja N, Prasad T (2015) Evaluation of the antimicrobial activity and cytotoxicity of phyto-genic gold nanoparticles. *Appl Nanosci* 5(5):595–602
- Sreelakshmi C, Datta K, Yadav J, Reddy B (2011) Honey derivatized Au and Ag nanoparticles and evaluation of its antimicrobial activity. *J Nanosci Nanotechnol* 11(8):6995–7000
- Stockert JC, Horobin RW, Colombo LL, Blázquez-Castro A (2018) Tetrazolium salts and formazan products in cell biology: viability assessment, fluorescence imaging, and labeling perspectives. *Acta Histochem* 120(3):159–167
- Strober W (2001) Trypan blue exclusion test of cell viability. *Curr Protoc Immunol*, Appendix 3, Appendix 3B
- Su C, Huang K, Li H-H, Lu Y-G, Zheng D-L (2020) Antibacterial properties of functionalized gold nanoparticles and their application in oral biology. *J Nanomater* 2020:1–13
- Suresh AK, Pelletier DA, Wang W, Broich ML, Moon J-W, Gu B, Allison DP, Joy DC, Phelps TJ, Doktycz MJ (2011) Biofabrication of discrete spherical gold nanoparticles using the metal-reducing bacterium *Shewanella oneidensis*. *Acta Biomater* 7(5):2148–2152
- Suzuki D, Kawaguchi H (2005) Gold nanoparticle localization at the core surface by using thermo-sensitive core-shell particles as a template. *Langmuir* 21(25):12016–12024
- Tao C (2018) Antimicrobial activity and toxicity of gold nanoparticles: research progress, challenges and prospects. *Lett Appl Microbiol* 67(6):537–543
- Tielens F, Santos E (2010) AuS and SH bond formation/breaking during the formation of alkanethiol SAMs on Au (111): a theoretical study. *J Phys Chem C* 114(20):9444–9452
- Tuersun P, Han X (2013) Optical absorption analysis and optimization of gold nanoshells. *Appl Opt* 52(6):1325–1329
- Turkevich J, Stevenson PC, Hillier J (1951) A study of the nucleation and growth processes in the synthesis of colloidal gold. *Discuss Faraday Soc* 11:55–75
- Venditti I (2019) Engineered gold-based nanomaterials: morphologies and functionalities in biomedical applications. A mini review. *Bioengineering (Basel)* 6(2):53
- Vidya S, Mutalik S, Bhat KU, Huilgol P, Avadhani K (2016) Preparation of gold nanoparticles by novel bacterial exopolysaccharide for antibiotic delivery. *Life Sci* 153:171–179
- Villiers C, Freitas H, Couderc R, Villiers MB, Marche P (2010) Analysis of the toxicity of gold nanoparticles on the immune system: effect on dendritic cell functions. *J Nanopart Res* 12(1):55–60
- Vimbela GV, Ngo SM, Frazee C, Yang L, Stout DA (2017) Antibacterial properties and toxicity from metallic nanomaterials. *Int J Nanomed* 12:3941
- Vinoj G, Pati R, Sonawane A, Vaseeharan B (2015) In vitro cytotoxic effects of gold nanoparticles coated with functional acyl homoserine lactone lactonase protein from *Bacillus licheniformis* and their antibiofilm activity against *Proteus* species. *Antimicrob Agents Chemother* 59(2):763–771
- Vistica DT, Skehan P, Scudiero D, Monks A, Pittman A, Boyd MR (1991) Tetrazolium-based assays for cellular viability: a critical examination of selected parameters affecting formazan production. *Cancer Res* 51(10):2515–2520
- Wadhvani P, Heidenreich N, Podeyn B, Bürck J, Ulrich AS (2017) Antibiotic gold: tethering of antimicrobial peptides to gold nanoparticles maintains conformational flexibility of peptides and improves trypsin susceptibility. *Biomater Sci* 5(4):817–827

- Walker T, Dumadag S, Lee CJ, Lee SH, Bender JM, Cupo Abbott J, She RC (2016) Clinical impact of laboratory implementation of Verigene BC-GN microarray-based assay for detection of gram-negative bacteria in positive blood cultures. *J Clin Microbiol* 54(7):1789–1796
- Wan W, Yeow JT (2012) Antibacterial properties of poly (quaternary ammonium) modified gold and titanium dioxide nanoparticles. *J Nanosci Nanotechnol* 12(6):4601–4606
- Wang S, Lu W, Tovmachenko O, Rai US, Yu H, Ray PC (2008) Challenge in understanding size and shape dependent toxicity of gold nanomaterials in human skin keratinocytes. *Chem Phys Lett* 463(1–3):145–149
- Wang SH, Lee CW, Chiou A, Wei PK (2010) Size-dependent endocytosis of gold nanoparticles studied by three-dimensional mapping of plasmonic scattering images. *J Nanobiotechnol* 8:33
- Wang P, Wang X, Wang L, Hou X, Liu W, Chen C (2015) Interaction of gold nanoparticles with proteins and cells. *Sci Technol Adv Mater* 16(3):034610
- Wang Z, Dong K, Liu Z, Zhang Y, Chen Z, Sun H, Ren J, Qu X (2017a) Activation of biologically relevant levels of reactive oxygen species by Au/g-C₃N₄ hybrid nanozyme for bacteria killing and wound disinfection. *Biomaterials* 113:145–157
- Wang L, Hu C, Shao L (2017b) The antimicrobial activity of nanoparticles: present situation and prospects for the future. *Int J Nanomed* 12:1227
- Wang SG, Chen YC, Chen YC (2018) Antibacterial gold nanoparticle-based photothermal killing of vancomycin-resistant bacteria. *Nanomedicine (Lond)* 13(12):1405–1416
- Wang J, Zhang J, Liu K, He J, Zhang Y, Chen S, Ma G, Cui Y, Wang L, Gao D (2020) Synthesis of gold nanoflowers stabilized with amphiphilic daptomycin for enhanced photothermal antitumor and antibacterial effects. *Int J Pharm* 580:119231
- Wani IA, Ahmad T (2013) Size and shape dependant antifungal activity of gold nanoparticles: a case study of *Candida*. *Colloids Surf B* 101:162–170
- Wimley WC, Hristova K (2011) Antimicrobial peptides: successes, challenges and unanswered questions. *J Membr Biol* 239(1–2):27–34
- Xing X, Ma W, Zhao X, Wang J, Yao L, Jiang X, Wu Z (2018) Interaction between surface charge-modified gold nanoparticles and phospholipid membranes. *Langmuir* 34(42):12583–12589
- Xue Y, Li X, Li H, Zhang W (2014) Quantifying thiol–gold interactions towards the efficient strength control. *Nat Commun* 5(1):1–9
- Yang X, Yang J, Wang L, Ran B, Jia Y, Zhang L, Yang G, Shao H, Jiang X (2017) Pharmaceutical intermediate-modified gold nanoparticles: against multidrug-resistant bacteria and wound-healing application via an electrospun scaffold. *ACS Nano* 11(6):5737–5745
- Yeom J-H, Lee B, Kim D, Lee J-K, Kim S, Bae J, Park Y, Lee K (2016) Gold nanoparticle-DNA aptamer conjugate-assisted delivery of antimicrobial peptide effectively eliminates intracellular salmonella enterica serovar typhimurium. *Biomaterials* 104:43–51
- Yu Y-Y, Chang S-S, Lee C-L, Wang CC (1997) Gold nanorods: electrochemical synthesis and optical properties. *J Phys Chem B* 101(34):6661–6664
- Yu Q, Li J, Zhang Y, Wang Y, Liu L, Li M (2016) Inhibition of gold nanoparticles (AuNPs) on pathogenic biofilm formation and invasion to host cells. *Sci Rep* 6:26667
- Yu Z, Li Q, Wang J, Yu Y, Wang Y, Zhou Q, Li P (2020) Reactive oxygen species-related nanoparticle toxicity in the biomedical field. *Nanoscale Res Lett* 15(1):115
- Yuan J-J, Schmid A, Armes SP, Lewis AL (2006) Facile synthesis of highly biocompatible poly (2-(methacryloyloxy) ethyl phosphorylcholine)-coated gold nanoparticles in aqueous solution. *Langmuir* 22(26):11022–11027
- Zawrah M, El-Moez S, Center D (2011) Antimicrobial activities of gold nanoparticles against major foodborne pathogens. *Life Sci* 8(4):37–44
- Zhang Y, Peng H, Huang W, Zhou Y, Yan D (2008) Facile preparation and characterization of highly antimicrobial colloid Ag or Au nanoparticles. *J Colloid Interface Sci* 325(2):371–376
- Zhang W, Li Y, Niu J, Chen Y (2013) Photogeneration of reactive oxygen species on uncoated silver, gold, nickel, and silicon nanoparticles and their antibacterial effects. *Langmuir* 29(15):4647–4651

- Zhang Y, Shareena Dasari TP, Deng H, Yu H (2015) Antimicrobial activity of gold nanoparticles and ionic gold. *J Environ Sci Health C* 33(3):286–327
- Zhao Y, Tian Y, Cui Y, Liu W, Ma W, Jiang X (2010) Small molecule-capped gold nanoparticles as potent antibacterial agents that target gram-negative bacteria. *J Am Chem Soc* 132(35):12349–12356
- Zhao Y, Chen Z, Chen Y, Xu J, Li J, Jiang X (2013) Synergy of non-antibiotic drugs and pyrimidinethiol on gold nanoparticles against superbugs. *J Am Chem Soc* 135(35):12940–12943
- Zheng K, Setyawati MI, Lim TP, Leong DT, Xie J (2016) Antimicrobial cluster bombs: silver nanoclusters packed with daptomycin. *ACS Nano* 10(8):7934–7942
- Zheng K, Setyawati MI, Leong DT, Xie J (2017) Antimicrobial gold nanoclusters. *ACS Nano* 11(7):6904–6910
- Zhou Y, Kong Y, Kundu S, Cirillo JD, Liang H (2012) Antibacterial activities of gold and silver nanoparticles against *Escherichia coli* and *Bacillus Calmette-Guérin*. *J Nanobiotechnol* 10(1):1–9
- Zhu Y, Ramasamy M, Yi DK (2014) Antibacterial activity of ordered gold nanorod arrays. *ACS Appl Mater Interfaces* 6(17):15078–15085